Draft Translation
Please refer to text of original report from University of Laval

Characterization and Evaluation of Tire-Roadway Interface Stresses

Pascale Pierre
Guy Doré
and
Laetitia Vagile

Report GCT-03-03

Submitted to the

Ministère des Transports du Québec

February 2003

TABLE OF CONTENTS

LIST OF FIGURES

LIST OF TABLES

LIST OF APPENDICES

1. INTRODUCTION

1.1. Project statement

This research project on characterizing and evaluating tire-roadway interface stresses was conducted subsequent to a study on the effects of tire width by the *Service des chaussées du Ministère des Transports du Québec*.[1] This research project consisted of in-depth experimentation conducted in a Quebec setting to satisfactorily apply the model described in the aforementioned study. The model evaluated tire impact on roadways and was based on the fact that contact pressure represents the average distribution of rib-roadway interface pressure.

A vehicle exerts force on the roadway via the rib-roadway contact surface. Contact pressures develop at this surface and affect how the roadway responds to the stresses applied. This study evaluated the factors that characterize load conditions at the road surface for tires commonly used on non-standard vehicles. These factors were determined for the inflation pressures recommended by tire manufacturers for various applied loads.

This research project was part of a special road licence review that considered allowable axle weights for non-standard vehicles. The issue was to evaluate the road-friendliness of different tire types and the roadway damage they may cause. In the special road licence regulation currently applied by the *Ministère des Transports*, axle weights allowed on non-standard vehicles using the road network are a function of axle spacing and tire width. The purpose of these requirements is to protect roadways from extreme high peak stress levels. Recent studies have shown that high pressure levels generated by rib-roadway contact cause roadway damage that is 80% to 200% higher than the amount of damage estimated by the current method, which assumes a maximum tire capacity of 10 kg/mm of tire width. A model was therefore developed to determine tire-roadway contact pressure based on tire type (tires with 5 or 6 surface ribs), inflation pressure, and load carried. Thus, based on load conditions and tire type, it is possible to evaluate how road-friendly a tire is as it moves along a roadway. The complexity of the tire-roadway interface phenomenon was addressed by including tire stiffness, contact surface, and contact pressure in the model. The experimentation conducted to validate this model should optimize the provisions related to allowable axle weights on heavy vehicles.

1.2. Objectives

The main goal of this research was to develop a tool for evaluating tire impact on roadways that would make it possible to set allowable axle weights that would be specified in the revised version of the special road licence regulation.

The experimental data gathered during this project validated the existing model. The project measured road response and road behaviour in relation to tire type, load condition, and the tire inflation pressure. Roadway deflections and distortions, both vertical and horizontal, were measured in response to various stresses in order to validate the theoretical calculations derived during the study conducted by the *Service des chaussées*.

[1] Quebec Ministry of Transportation Roadway Service

The specific objectives of the project were:

Instrumentation and measurement

- To instrument the *section d'analyse de l'agressivité des véhicules lourds* (AVL) of the *Site expérimental routier de l'Université Laval* (SERUL)[2] in order to measure roadway response under various stresses;
- To measure deflections and distortions at critical levels in the roadway;
- To take three-dimensional measurements of the pavement distortions caused by a heavy vehicle in movement in order to evaluate roadway behaviour at the tire-roadway interface;

Validating the model

- To obtain the experimental data on the instrumented roadway needed to validate the existing contact pressure model;
- To provide a roadway tire impact evaluation tool that would set allowable axle weights to be specified in the revised version of the special road licence regulation.

1.3. Methodology

The project involved the following steps:

1. Updating the literature review on the effect of tire width and on the measurement of roadway pavement distortions;
2. Instrumenting the roadway in the *section d'analyse de l'agressivité des véhicules lourds* (AVL) of the *Site expérimental routier de l'Université Laval* (SERUL) in order to obtain data related to vehicle movement on the roadway, both with respect to tire impact on the roadway and roadway behaviour following this impact;
3. Measuring deflections and distortions at various critical levels in the roadway;
4. Presenting and analysing experimental data to validate the model developed by the *Service des chaussées du Ministère des transports du Québec*.

2. LITERATURE REVIEW

This knowledge review starts with a brief update of the review conducted as part of the study by the *Service des chaussées du Ministère des transports du Québec* (Prophète, 1999). It then discusses the various types of instrumentation capable of measuring tire-pavement interface pressure.

2.1. Updating the literature review

Tire-roadway interface stresses have been the subject of several studies over the past 15 years, which have resulted in several articles. The studies conducted to date (Lippmann, 1985; Markshek *et al.*, 1986; Tielking and Roberts, 1987; Beer *et al.*, 1997; Siegfried, 1998) have led to the following conclusions:

[2] road-friendliness analysis section of the Laval University road research site

- Vertical contact stresses under a tire are not uniform. The distribution of these stresses depends on a tire's design;
- Vehicle speed does not affect vertical stresses but does affect longitudinal stresses;
- When a tire is static, the friction between the tire tread and the road surface develops tangential forces directed inward toward the centre of the tire-roadway contact area;
- When a tire is moving, longitudinal shear develops at the centre of the contact surface (Figure 1).

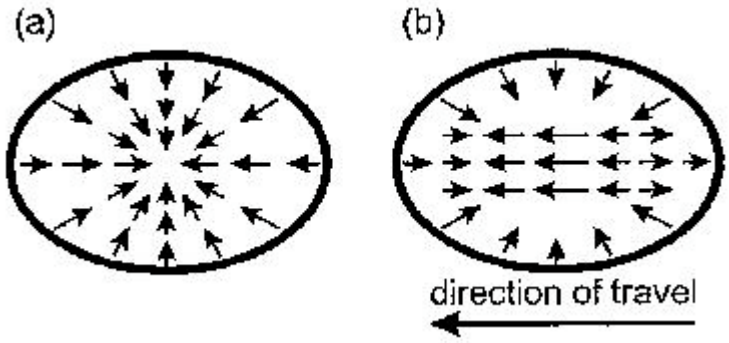

Figure 1 - Contact stresses on the roadway surface around the edge of a tire footprint for (a) a static tire and (b) a free wheel (Tielking and Roberts, 1987)

The research presented in this part discusses various approaches that have been used to determine how the tire-pavement interface affects roadway behaviour.

The distribution of forces and stresses in a roadway is a function of roadway stiffness and thickness as well as load amplitude, axle type and configuration, and tire pressure. The study by Sebaaly (1992) showed how inflation pressure, tire type, axle load, and axle configuration affect the response of flexible asphalt concrete pavement. The study was based on parameters related to roadway fatigue (cracks). A roadway's lifespan (expressed as a number of standard load repetitions) was calculated based on relationships drawn from the study by Finn *et al.* (1986). A theoretical analysis was first performed using the linear elastic multilayer model. The following structures were chosen: a shallow structure consisting of 15 cm of asphalt concrete and 20 cm of aggregate over the subgrade, and a deeper structure consisting of 25 cm of asphalt concrete and 25 cm of aggregate over the subgrade. The tires used were: the Radial 11R22.5 (dual tires) and a wide-based tire 385/65R22.5 (single tire). The inflation pressures were 725 and 895 kPa and the loads were 45, 75, and 98 kN per axle for the dual tires and 45, 75, and 89 kN per axle for the wide tires. The theoretical analysis showed that:

- Contact pressures are not uniform, and their distribution depends on load, tire type, and inflation pressure;
- For both the Radial tire and the wide-based tire, increasing the tire inflation pressure increases traction stresses by less than 10% for the three load levels.
- Axle loads have a much greater effect than inflation pressure for both tire types; increased loads cause increased stress;

Trials were conducted in situ on roadways with the same structures as those used for the theoretical analysis. Stress gauges installed at the pavement base layer of two experimental road sections were used to collect data. Along with the roadway response parameters, temperature readings were taken to bring all stress measurements to a standard 21°C. This study produced the following findings:

- The stresses calculated and measured for the 11R22.5 tire in a dual-tire configuration were the lowest for both sections of roadway;
- Tire inflation pressure does not lead to significant differences in the stresses measured and calculated. Inflation pressure does not therefore appear to be a factor that affects how roadway structures with 15 to 25 cm of asphalt concrete pavement respond;
- The response to single tires is always higher than to dual tires. The 385/65R22.5 tire (single configuration) generates much greater stress than other tires;
- Traction stresses under single axles are greater than under tandem axles. Similarly, with respect to fatigue cracks, tandem axles are less damaging to the roadway than single axles.

Another study (Christison, 1990) also demonstrated and confirmed that tire pressure has little effect on roadway response. This experimental study evaluated the effect of tire pressure on superficial distortions, interfacial traction stresses in asphalt concrete pavement, and superficial compression stresses. Pavement behaviour in response to two-wheel load configurations with three different tire pressures was measured and compared to the findings obtained in simultaneous trials with a standardized load. In general, the extent of behaviour variability that results from modifying the tire pressure is limited. No specific trend with respect to pavement behaviour in response to variations in tire pressure could be identified.

More recently, other researchers have used tire pressure variation systems such as VTP, Variable Tire Pressure (Owende *et al.*, 2001) and CTI, Central Tire Inflation (Douglas *et al.*, 2000) to study the stresses that heavy vehicles cause as they move on flexible roadways. In the study conducted by Owende *et al.* (2001), the types of damage studied were primarily fatigue cracks and rutting, respectively caused by traction stresses, which are at maximum levels at the base of the pavement layer, and vertical compression stresses at the topgrade. Thus, interfacial roadway stresses and the stresses at the base of the structure were created by a heavy vehicle in movement to evaluate roadway lifespan. Three pressure cells were installed at the topgrade and three others were installed at the pavement base layer and placed such that each measured the pressure under a passing wheel at three different locations (external, middle, and internal part of the tire). A fourth cell was installed at the surface to measure the pressure between the wheels. The tire-pavement contact area was measured concurrently to capture the reduction in contact surface area that occurrred as inflation pressure was increased for a given load. Based on this study, the authors came to the following conclusions:

- Lateral stresses caused by the front turning wheel of a heavy vehicle in movement are the strongest and are the primary factor reducing the lifespan of a flexible roadway on compressible soil (peat).

- Lateral stresses control the initiation of fatigue cracks but longitudinal stresses control their growth. Longitudinal stresses increase significantly with increased tire pressure. Low inflation pressure is therefore recommended for all wheels.
- The roadway only responds at the surface to use of the VTP system. The sole effect is to reduce the number of fatigue cracks, since varying the tire inflation pressure only affects stresses at the pavement base layer.
- The only way to reduce the phenomenon of rutting, which results from forces at the topgrade, would be to reduce loads.

Similarly, laboratory experiments were conducted to measure tire contact pressures on a roadway. The study by Yap (1989) measured tire contact pressures in order to better understand tire design factors (tire type) and operational factors (inflation pressure, axle load). Data were collected for set loads and inflation pressures by rolling tires slowly (quasi-static condition) on a steel plate over a stress gauge that itself moved laterally to obtain readings across the tire's entire width. Tire loads and tire speeds generate forces at the tire-pavement interface and have three components: X (longitudinal), Y (lateral), and Z (vertical). The contact forces are directed longitudinally and laterally, and they result from the change in tire shape at the tire-pavement interface. These forces generally have a lower amplitude than those developing vertically. The study focused primarily on the pressure exerted vertically by a loaded tire. These pressures are not uniform, both with respect to the width and length of the tire footprint (Figure 2).

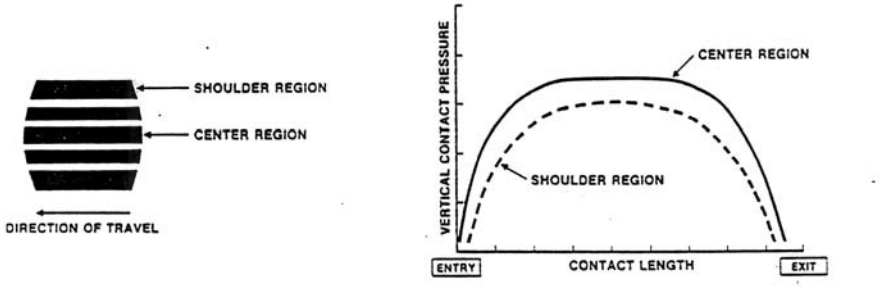

Figure 2 – Vertical contact pressures along the tire print

On the edge of the tire footprint, the pressure gradually increases and then decreases past the centre of the print. The central area shows the same phenomenon with a maximum level at the centre of the contact surface. The distribution of pressures over the tread width depends on the tire's load but also on its design. One of the primary factors is tire width. Finally, the study concluded that load variations affect tire contact pressures significantly more than inflation pressure variations do.

Finally, some research has examined how tire type affects road damage. Al-Qadi *et al.* (2002) compared the damage caused by a new wide-based tire and a conventional tire. To quantify the effects these tires have on the roadway, an experimental program was conducted on the Virginia Smart Road site constructed in 1998. The roadway structure was instrumented to measure

distortions, pressure under the tires, and temperature. Trials were conducted during three different periods: May 2000, November 2000, and July 2001. The study's findings showed that:

- The new wide-based tires cause the same horizontal stresses under the pavement layer that dual conventional tires do. Fatigue damage is equivalent for both tire types.
- Vertical compression stresses are higher for wide-based tires than for conventional tires, but this difference diminishes with structure depth and becomes negligible at the base of the foundation layer.
- Surface contact pressures for the new tires are lower than for conventional wide-based tires.
- The front turning wheel appears to cause the greatest horizontal stresses. The authors therefore recommended using this type of configuration for predicting roadway lifespan.

2.2. Review of instrumentation capable of measuring pressure at the tire-roadway interface

This part of the literature review examines various systems for measuring pressure at the tire-pavement interface. Since the experimental program involved performing this type of measurement, it was considered necessary, as a first step, to undertake a detailed review of existing measurement systems to ensure that the research would take knowledge in this field into account. The systems presented below were selected to represent a broad range of the various systems developed to date to measure tire-roadway interface stresses, and, more especially, contact pressures that a vehicle in movement may exert on a roadway surface.

The first system is a VRSPTA prototype (Vehicle-Roadway Pressure Transducer Array) that was developed to measure stress at the tire-roadway interface as a vehicle moves (de Beer, 1996). The device was designed to simultaneously measure vertical, lateral, and longitudinal stress as well as the distribution of stress transferred to the road surface by a moving wheel. These stresses and stress distributions are measured across a tire's entire width. To do so, an arrangment of pressure cells containing distortion gauges was installed in rows at right angles to the direction of vehicle movement. As a wheel passes over a stress gauge, the latter undersent a high-frequency screen.

Through their design, the pressure cells, consisting of distortion gauges, had to meet two objectives: they had to provide maximum sensitivity in the vertical, lateral, and longitudinal directions, and they had to be able to withstand the loads of passing vehicles. The cells were therefore manufactured from high-tensile steel and subsequently underwent heat treatment. The cells' measurement surface was 73.9 mm². A surface 15 mm by 15 mm was monitored to calculate the stress. The stiffness of the area around each cell had to be similar to the cell itself in order to avoid altering the distribution of the tire load. In the case of the VRSPTA, an array consisting of 100 m² of grade 5 steel squares was manufactured. These squares were as stiff as the measurement cells laterally and longitudinally but are more stiff vertically. The array of squares consisted of three different sections subsequently screwed together. Direct current and switches were used to change between the three directions of measurement. Before being installed, each pressure cell was calibrated individually with a device able to apply predetermined loads in each of the three directions of measurement. A frequency modulation recorder was connected to the analog signal output from the distortion gauges to record the data. Macro-switches were installed just before and just after the pressure cells. These macro-switches act as triggers when a wheel passes. The trial's findings demonstrated that direct measurement of a vertical load by the VRSPTA underestimated the applied load by approximately 25%. This discrepancy resulted from some differences between the stress cells and the cells in the perimeter array. First, the lower

vertical stiffness of the instrumented cells caused these cells to undergo greater deflection than those in the perimeter array. This deflection contributed to redistributing the load toward the cells in the array. Therefore, to correct this problem, it is recommended that cells in the perimeter array and the instrumented cells be the same size and constructed of the same materials. Furthermore, to facilitate data collection, it is recommended to have a calibration system and data collection system for each direction of measurement.

In Denmark, Krarup (1992) used a CSC (Contact Stress Cell), which is a dual-diaphragm cell designed to record vertical stress at the tire/pavement interface. This cell acts like a rock in the material in which the stress is measured. This device consists of a distortion gauge surrounded by a fine membrane, with an incompressible layer of liquid and a surface membrane placed above (Figure 3). Installing such cells involves drilling a hole in the asphalt the same size as the cell such that the surface membrane is flush with the pavement. The cell is secured with resin. The surface of the cell must be small enough for the tire to cover it completely as it passes over. To avoid asymmetrical distortion of the surface membrane, which causes erroneous findings, the cell must be be approximately 5 cm in diameter (standard for a 12R22.5 tire) and the surface membrane must be in total contact with the tire.

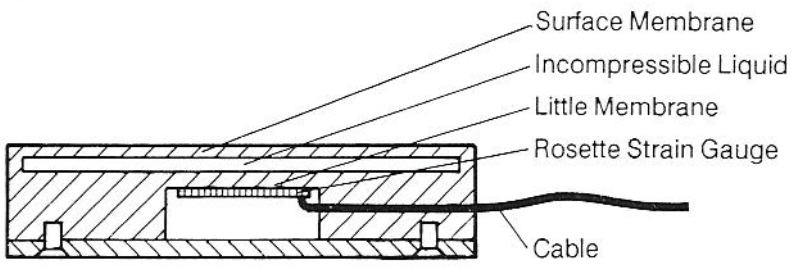

Figure 3 – Dual-diaphragm cell (Krarup, 1992)

Measuring the stress applied to the soil must be performed such that the stress cells placed in the soil do not modify the current state of stress. The cells must therefore meet certain characteristics in relation to the soil in which they are placed. They must:

- have a diameter at least 50 times larger than the largest grain of soil;
- be comparable in density to the surrounding soil;
- not be placed near large particles of soil, because this may cancel the stress concentration effect;
- be water resistant and have very durable wires.

Two types of these cells exist. The first one is the diaphragm pressure cell, which consists of a rigid circular diaphragm supported by an integral stiff-edged ring. Pressure compresses this diaphragm. Electrical resistance gauges or other types of distortion measurement sensors are attached to the inside surface of the diaphragm. The second type is the hydraulic pressure cell, which consists of two circular metal plates glued together around their circumference. The cavity thus created is filled with mercury. The total stress on the cell is balanced by equivalent pressure induced in the internal liquid. These two types of cells are illustrated in figures 4 and 5. Table A1

in Appendix 1 shows the costs and availability of various brands of pressure cells. These cells vary between 2 and 7 mm in diameter, depending on the brand and model.

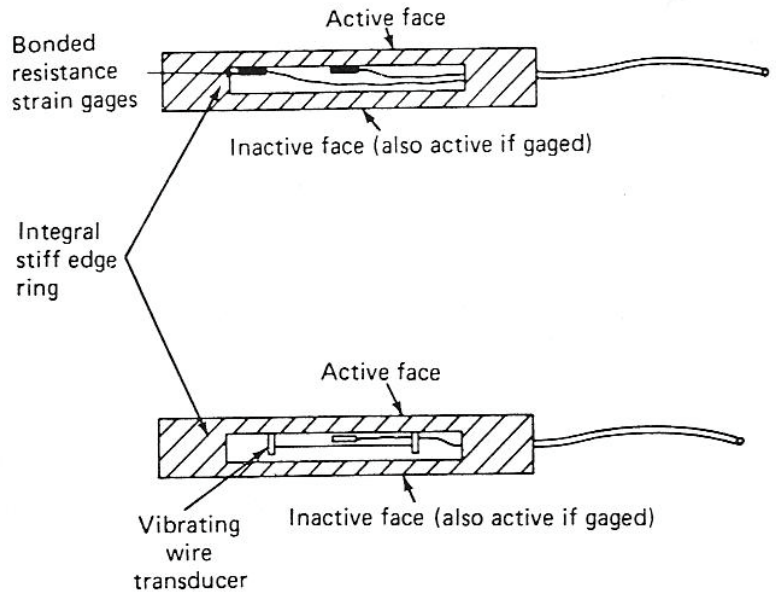

Figure 4 – Diaphragm pressure cell (U.S. Department of Transportation)

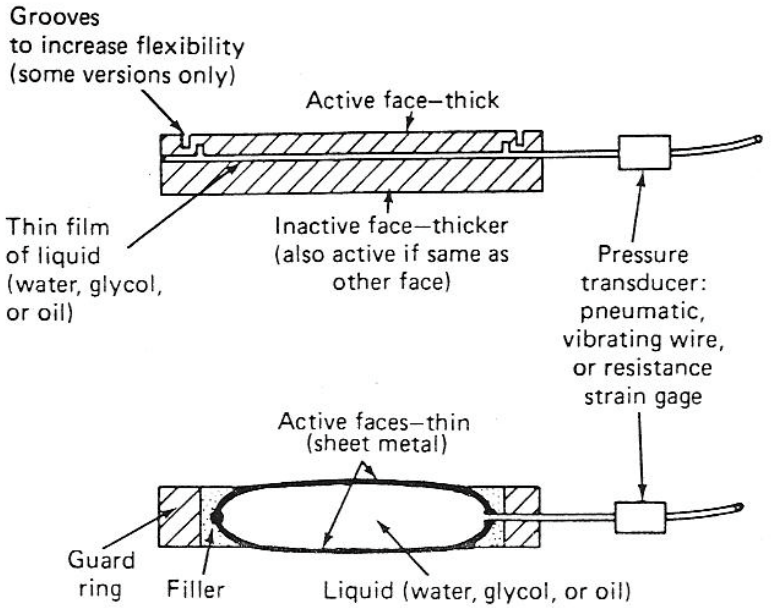

Figure 5 – Hydraulic pressure cell (U.S. Department of Transportation)

Other systems exist for measuring stress at the tire-pavement contact surface. The system described by Lippmann (1985) is 12 m long and consists of a bed in which a stress transmitter (5 mm by 5 mm) is placed. This transmitter measures interfacial pressure and horizontal stresses in the direction of, and perpendicular to, a vehicle's movement. The measurement device is designed so that the transmitter can be moved laterally in the roadway to measure the pressure at various points across a tire's width. To determine the force that develops at the tire-pavement interface, a tool was designed to measure this force at 10 points across a tire's width (Howeel *et*

al., 1986). Each pressure sensor measures 1.27 cm by 1.27 cm. The device is designed such that, when the top plate is installed, it arrives flush with the sensors. It should be noted that this instrument is designed for conducting trials in the laboratory because the wheel is held by a U-shaped support and is not attached to a truck.

Finally, several other methods exist for measuring pressure distribution on the tire-pavement contact surface. Piezoelectric sensors have now been developed to measure pressure distribution caused by an object in movement, and these seem to provide realistic pressure distribution readings. However, it appears that the most successful instrument in the tire industry for measuring such pressures is the triaxial pressure cell. The Texas Transportation Institute recently created its own pressure cell. It is the smallest on the market (11.4 mm²). This cell has two main advantages over pressure sensitive films, namely, that it measures shearing stress and that the signal from the pressure cell responds to dynamic tire contact pressure. In one study (Tielking and Abraham), 10 pressure cells were aligned across a tire's width. This assembly was secured using a box (508 mm x 508 mm x 12.7 mm) matching the tire contact surface. The device measured stress distribution across a tire's width. Each pressure cell was equipped with three distortion gauges, each wired to a channel. A change in voltage corresponded to a change in pressure. This assembly was designed for laboratory use, with the tire attached to a U-shaped support and not a truck. Figures 6 and 7 show this assembly. Data collection was performed by a computerized monitoring unit. The wheel was moved laterally across the contact plate to obtain readings across a tire's entire width. To measure normal pressure, initial load-free readings were obtained for each pressure cell. The tire load was then applied by moving the plate containing the cells toward the tire. Finally, the différences between the two voltage readings and each cell's line of calibration were used to determine the normal pressure.

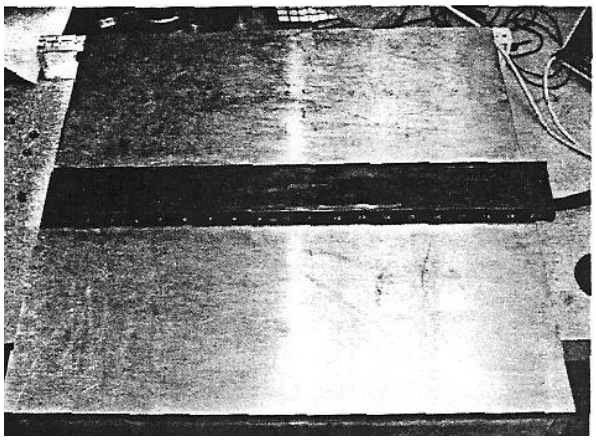

Figure 6 – Plate for measuring tire contact pressure (Tielking and Abraham)

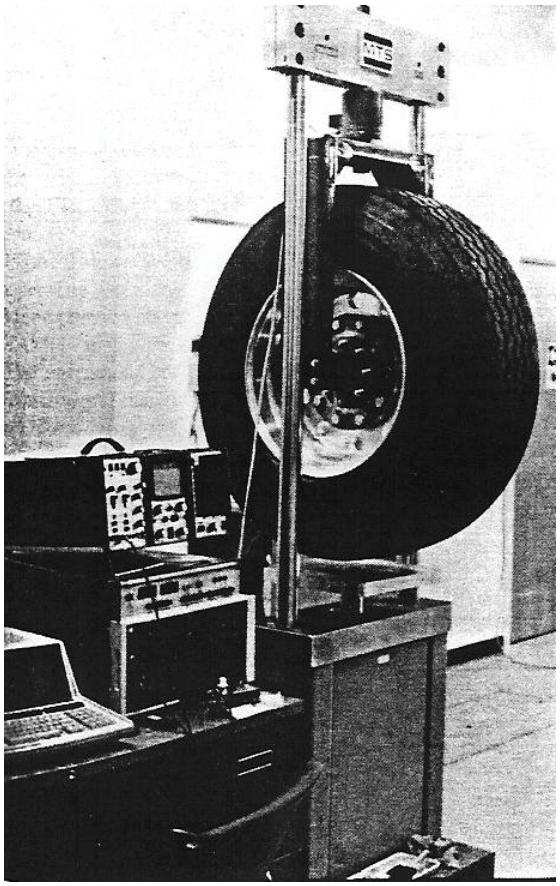

Figure 7 – U-system tire assembly (Tielking and Abraham)

This literature review was not exhaustive, quite the contrary. It simply elaborated on the literature review conducted for the *Service des chaussées'* study by adding recently completed work. It focused mainly on compiling various pieces of research on measuring roadway contact pressures. This review assisted and supported the selection of the measurement systems created and used during this study.

3. ROADWAY INSTRUMENTATION

The objective of this study's experimental program was to obtain data on vehicles in movement, both with respect to tire impact on the roadway and the roadway's behaviour in response to this impact. The existing instruments in the AVL section of SERUL measured distortions at various critical levels in the roadway. The AVL section is equipped with fiber-optic distortion gauges that measured traction distortions at the pavement base, as well as multilevel deflectometers that measured vertical distortions at various levels in the roadway. In addition, fiber-optic distortion gauges installed in a slab placed in the pavement of the roadway measured distortions 25 mm below the surface. A series of distortion readings taken in three directions—vertical, longitudinal, and transversal—was obtained across a tire's width.

3.1. Presenting the research site

SERUL is located in the Montmorency Forest at kilometre 103 of highway 175. The site is a new section of forestry road 33 located 3.3 km east of highway 175. The project trials were conducted

on the 100-metre long AVL section of this road laboratory. The roadway structure at this location consists of (Figure 8):

100 mm of asphalt concrete that constitutes the roadway pavement;

200 mm of GM20;

480 mm of GM 112;

1,370 mm of silty till. This material is the soil that supports the roadway and is the first layer of natural soil under the infrastructure.

Test boring then revealed 450 mm of wood and a final 270 mm of sandy silt.

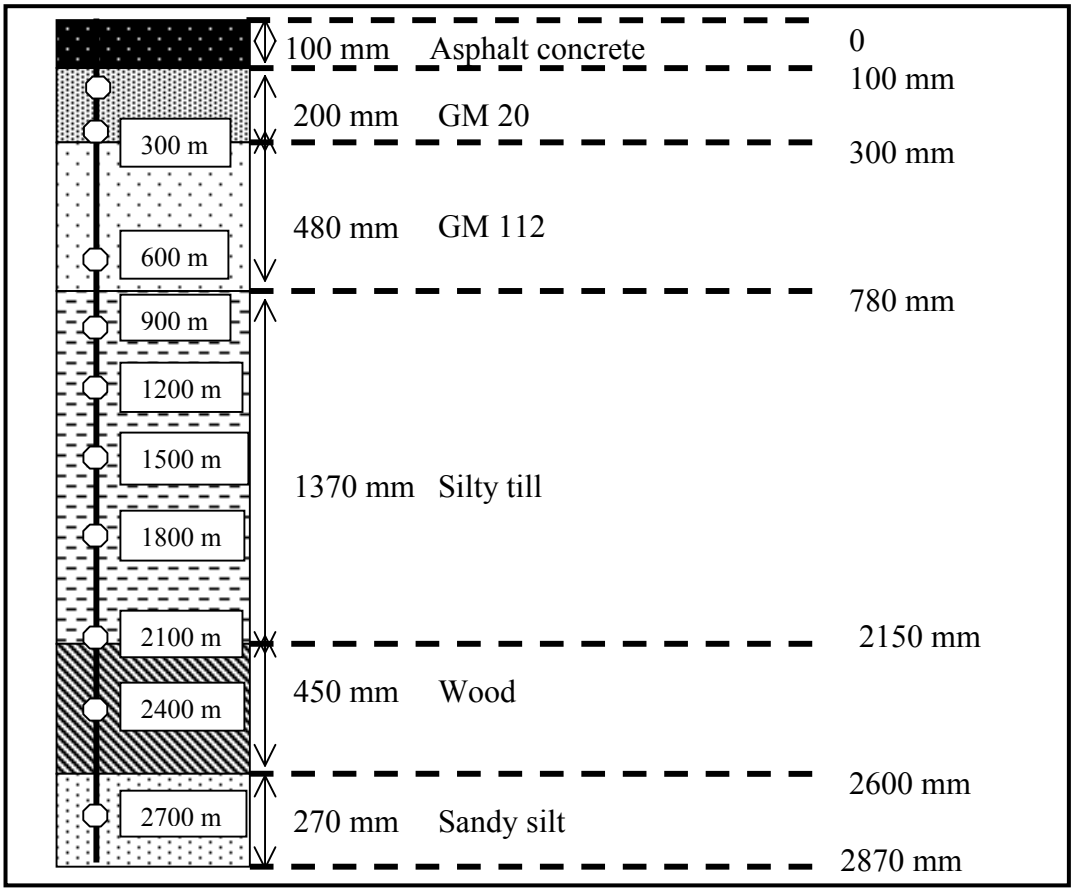

Figure 8 -- Roadway structure of the AVL section of SERUL
(⎔ thermistors)

3.2. Instrumentation for measuring deflections and distortions in the roadway

The AVL section of SERUL contains the following instrumentation installed in the roadway to measure distortions and deflections at various levels: three distortion gauges and a multilevel deflectometer placed as indicated in Figure 9.

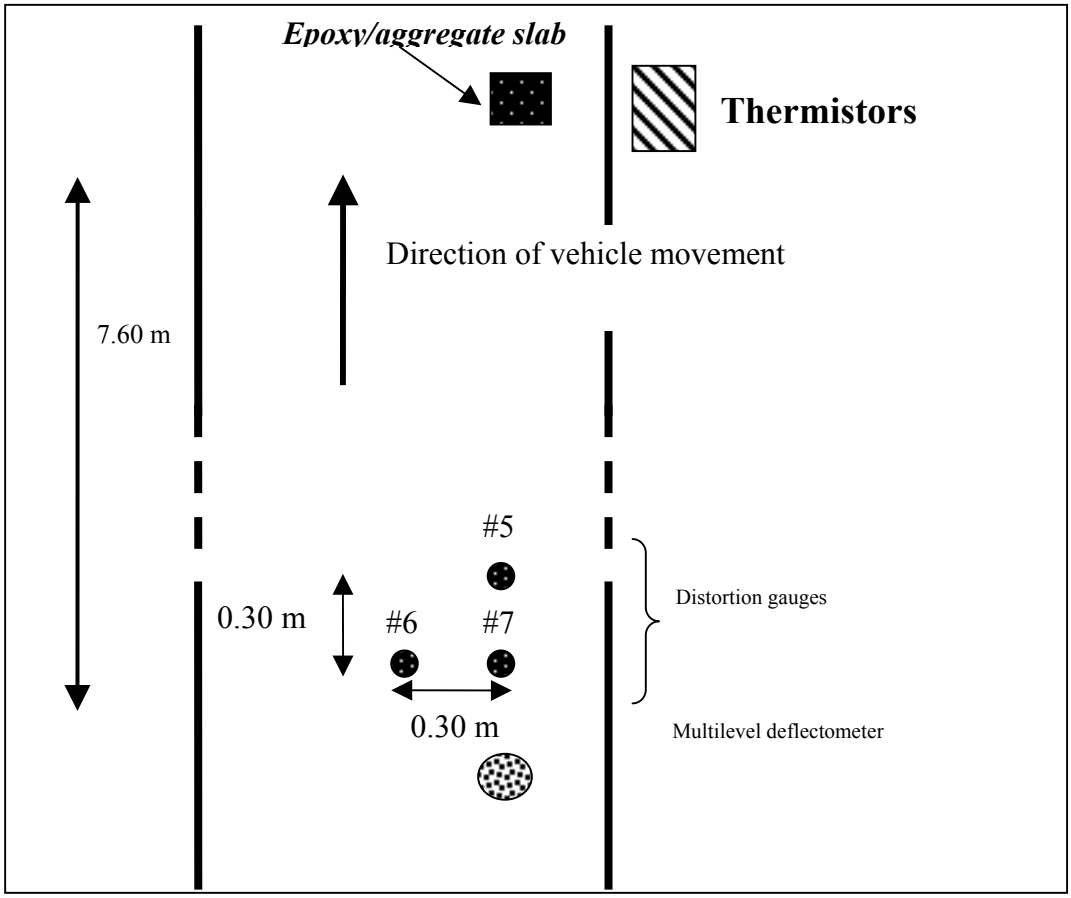

Figure 9 – Placement of instrumentation on the AVL section of SERUL

The fibre-optic distortion gauges numbered 5, 6, and 7 on Figure 9 measured horizontal distortions at the pavement base. Gauges 6 and 7 measured longitudinal distortions and gauge 5 measured transversal distortions. These gauges were constructed as follows: each gauge was first glued into a heavy-duty plastic tube. The material making up the plastic tube was chosen to be stiff enough to protect the gauge while also being slightly less stiff and slightly more resistant to rupture than most asphalt mixes. In this way, the tube did not significantly affect the force distribution in the layer of asphalt concrete. Each gauge was then glued to the base of an asphalt cylinder constructed in the laboratory. The cylinder diameter was kept small (58 mm) to minimize discrepancies in the behaviour of the layer of asphalt concrete, The asphalt mix used to construct the cylinder was selected to have the same properties (density and stiffness) as the layer of asphalt concrete in which it was placed. The shape of the gauges was printed onto the base of the cylinder when this was constructed, and a groove was cut into the side of the cylinder to accommodate the fibre-optic wires. Figure 10 shows this device schematically. The instrumented cylinders were then placed in 60 mm diameter holes drilled in the roadway and then sealed there. This situated the gauges at a depth of 100 mm, i.e. at the pavement base (Figure 11).

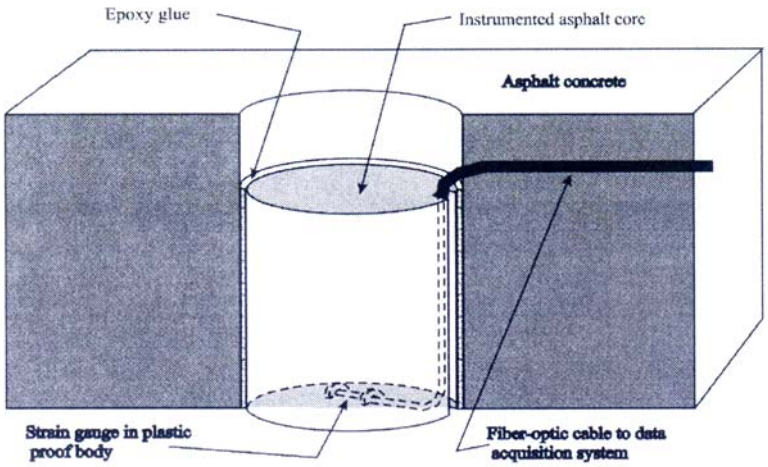

Figure 10 – Schematic illustration of an asphalt concrete cylinder instrumented with a distortion gauge

The multilevel deflectometer consisted of three leads whose extremities were screwed to plates located at the interfaces between the various levels of the roadway. Each lead was covered with a flexible tube to reduce friction between the lead and the surrounding soil. The plates were placed 300 mm, 800 mm, and 1,100 mm from the surface in a 150 mm diameter hole drilled in the roadway (Figure 11). A fourth lead was anchored at 2,500 mm and served as a control because, due to its depth, it was assumed that the plate anchoring this lead did not experience any movement. Thus, it was felt that movement of the sensor at the end of this lead (deflectometer 1) indicated total roadway deflection, while the other sensors measured the relative deflections at various levels in the roadway. The multilevel deflectometer also included a movable read head consisting of four fibre-optic movement sensors supported by the leads. This was set up and removed every day that readings were taken (Figure 12).

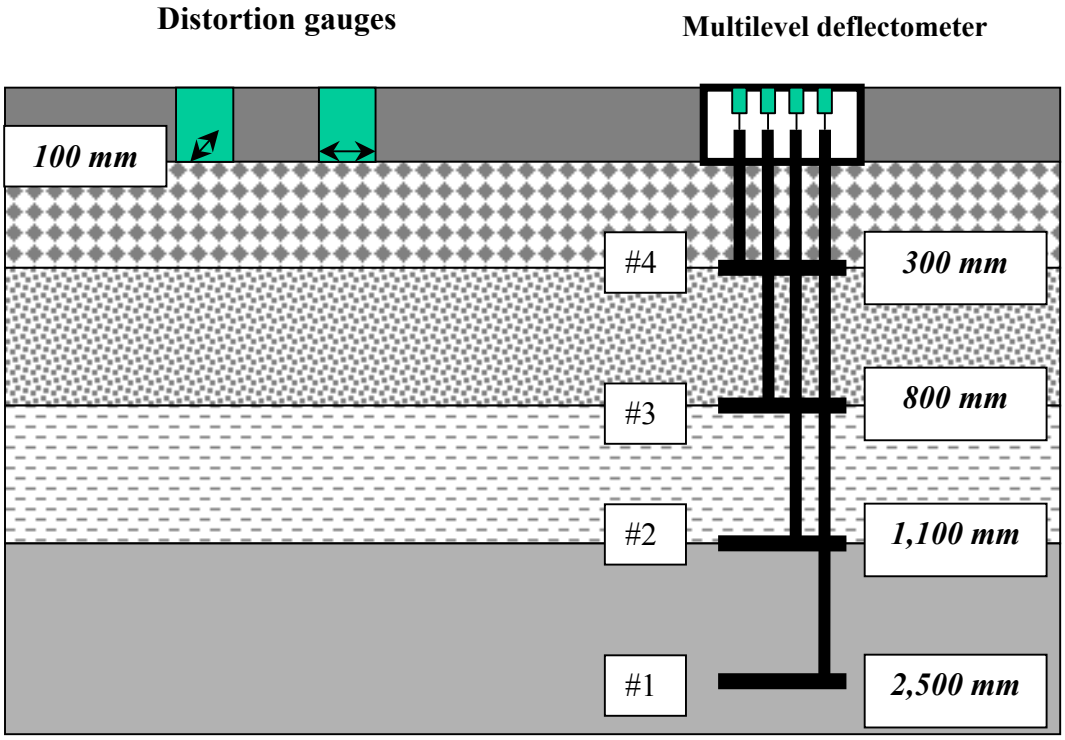

Figure 11 – Depth of the distortion gauges and multilevel deflectometer plates

Figure 12 - Multilevel deflectometer read head disasssembled

3.3. Instrumentation for measuring distortions in the pavement

To quantify tire impact on the roadway, distortions readings were taken at a depth of 25 mm, which is where maximum shear stresses occur. These readings were taken using an instrumented slab. Designing this instrumented slab involved choosing materials and conducting trials in the laboratory to simulate the experimentation subsequently conducted on the SERUL site.

3.3.1. Determining and characterizing the mix

An epoxy/aggregate mix was manufactured:

- To reproduce the heterogeneity of an asphalt concrete, i.e. an aggregate bound in a matrix, so that the composite material in the slab responded as much as possible like a conventional pavement;
- To eliminate as much as possible the phenomenon of asphalt concrete creep as temperatures increased, or, in other words, to neutralize the asphalt concrete's viscoelastic behaviour, since the trials were conducted during the summer under quasi-static conditions.

To optimize the final mix, several formulations were prepared with different types of epoxy and granulometry (Table 1). Mixes 3, 5, 6, and 7 were prepared with Sikadur binder 52 (E=1.80 Gpa) and mix 4 with Sikadur binder 35 (E=2.41 Gpa). Mixes 3, 4, and 7 had full range of granulometry while mixes 5 and 6 lacked fines particles (granulometry > 80 μm).

Table 1 - Description of the epoxy/aggregate mixes

Mix #	Binder	Granulometry	V_{epoxy} / V_{solid}	Goal
3 and 8	Sikadur 52	Full	20.8 %	Optimum Proctor
4	Sikadur 35	Full	20.8%	Optimum Poctor
5	Sikadur 52	> 80 μm	29.3%	Saturation
6	Sikadur 52	> 80 μm	33.3%	Supersaturation
7	Sikadur 52	Full	31.58%	Saturation

Compression trials were conducted on each sample to determine the modulus of the mix. The findings obtained are shown in Appendix 2. Mixes 3 and 5 had the weakest moduluses, i.e. the closest to that of an asphalt concrete. However, producing a slab with mix 5 would have required sifting at 80 μm, which is why mix 3 (Sikadur binder 52) was selected for producing the final slab. Compression trials at various temperatures were then conducted to determine the modulus of samples 3 and 8. The findings are shown in Appendix 2. The mix had a relatively stable modulus between 5°C and 20ºC (approximately 13 GPa) but the modulus was much weaker at 40ºC (approximately 6 GPa).

3.3.2. Constructing an initial epoxy/aggregate slab

An initial slab was constructed to test the instrumentation under load conditions and to check the operation of the fibre-optic distortion gauges. Three fibre-optic gauges were installed to measure distortions in three directions (vertical, longitudinal, and transversal). The size of the slab and the placement of the gauges are indicated on the layout in Appendix 3. Compression trials were conducted on the slab to check how the distortion gauges responded in relation to the point of load application. These trials were conducted using an Instron press equipped with a 150 kN load cell. Several loads were applied, and for each one, distortion readings were taken with the vertical gauge and the horizontal gauge by varying the distance between the gauge/centre and the press load head. The findings from this trial (Figure A3.1 in Appendix 3) showed that further from the load point, whether vertically or horizontally, distortion decreases significantly. A second series of trials was then conducted with a piece of truck tire placed between the instrumented slab and press load head (Figure 13). The purpose of these trials was to determine whether the gauges were sufficiently sensitive to show differences in distortion between a tire's grooves and ribs. The findings of these trials, presented in figures A3.2 and A3.3 in Appendix 3, proved satisfactory because the graphs show that reduced distortions correlate with the tire grooves.

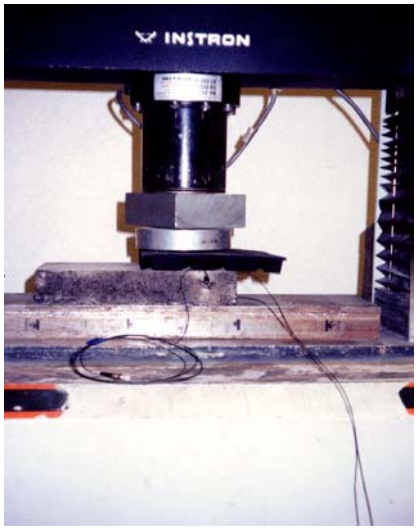

Figure 13 - Compression trial with a piece of tire placed between the slab and the load head

3.3.3. Constructing an instrumented epoxy/aggregate slab

After constructing an initial slab, the next step in the preparations for the summer trials was to design a mold for producing the slab and to design the components needed to install it on the SERUL site. A steel mold (Figure 14) was designed to contain the epoxy/aggregate mix. The mold-mix combination made up the final trial slab. Its dimensions were 2' long (609 mm), 1' wide (304.8 mm), and 4" deep (101.6 mm).

Figure 14 – Mold for the instrumented slab

The final instrumented slab was constructed as follows:

- A first layer of 75 mm of epoxy/aggregate mix was poured into the mold;
- Grooves for the horizontal gauges (longitudinal and transversal) were cut out with a saw. As well, holes were drilled in the material (subsequently filled with epoxy) for the gauge wires to reach the groove under the mold.

The next step consisted of pouring the remaining 25 mm to achieve the slab's full thickness. To install the vertical gauges, holes were drilled in the bottom of the mold to allow the extermities of the gauges to extend 75 mm from the base of the slab. These holes were also subsequently filled with epoxy.

The gauges were initially to be placed as indicated on Figure 15. However, because the fibre-optic gauges proved extremely fragile, several were damaged when they were placed in the epoxy/aggregate slab. Therefore, the slab's initial measurement device was modified to ensure that uniform readings were taken all along the slab.

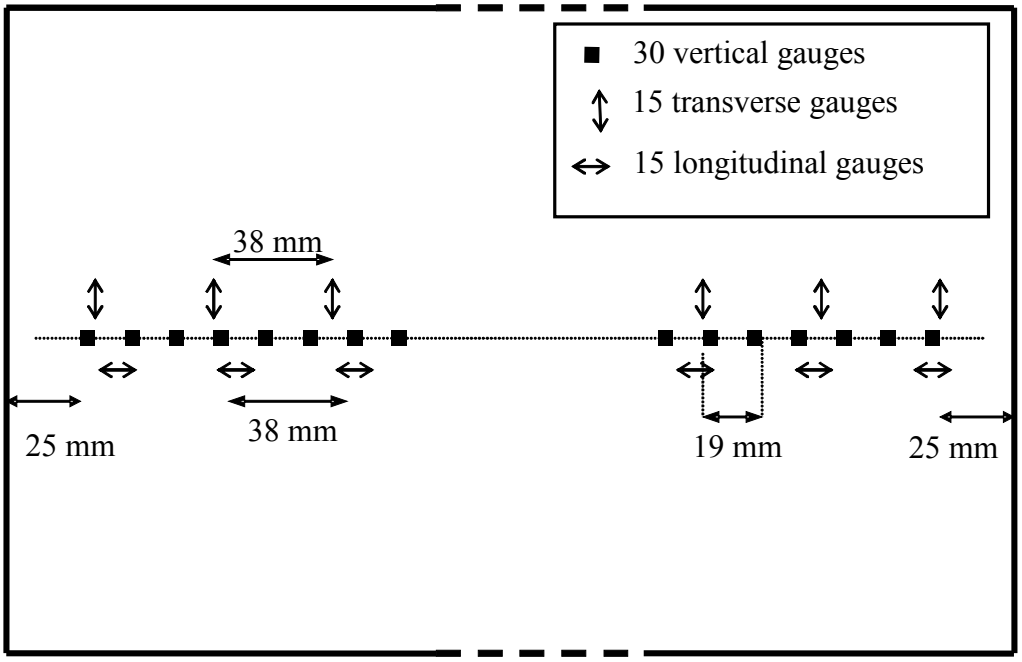

Figure 15 – Initial placement of the gauges in the epoxy/aggregate slab

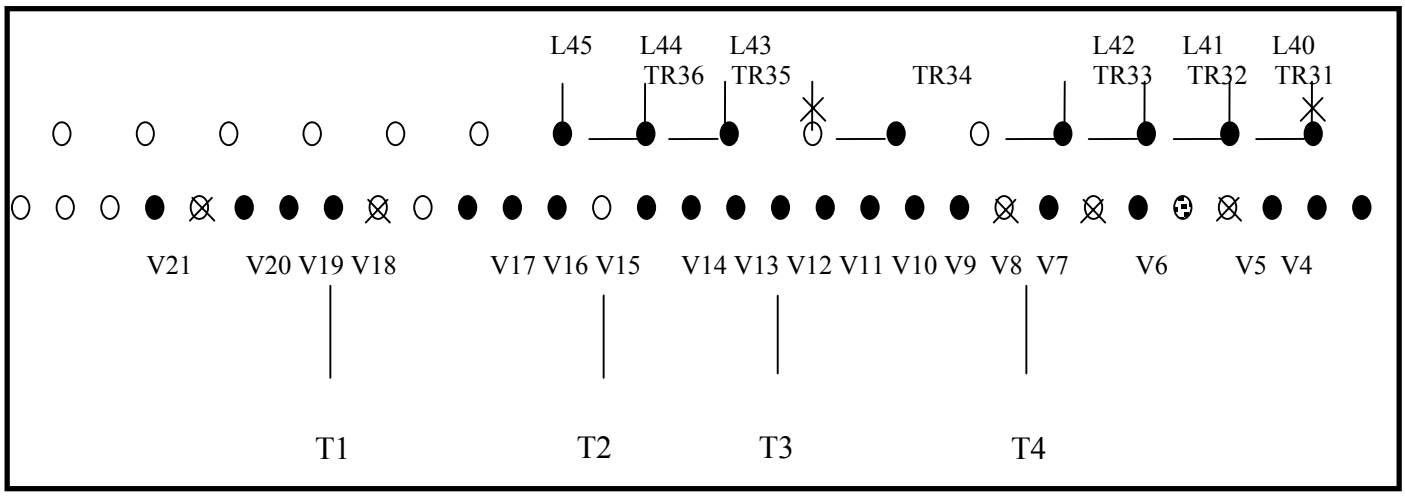

Figure 16 - Final placement of the gauges in the slab (V: vertical gauges, TR: transversal gauges, and L: longitudinal gauges)

The final device used to collect data during the summer trials is shown in Figure 16. The operational gauges are shown in black and the defective ones in white.

The slab was instrumented with four thermistors, identified T1 to T4 on Figure 15, to take temperatures readings at various points in the slab. These thermistors were placed at the same level as the distortion gauges. But the AVL section first had to be equipped with a device to support the slab during the summer trials. A steel support base was used to secure the slab-mold assembly in the roadway. Installing the support base involved the following steps:

- Digging a hole 4’ long (1,219 mm), 3’ wide (914 mm), and 2’ deep (609 mm) in the roadway (Figure 9);
- The support base was placed in the hole and maintained in position by the roadway as indicated in Figure 17;
- The cavity was then filled with concrete and levelled flush with the roadway surface. Using concrete ensured the stability of the support base by eliminating any risk of puncture by moving trucks;

The instrumented slab was installed in the support base (Figure 18) every day that readings were taken. Outside the trial periods, the instrumented slab was replaced by another steel plate that was strong enough for the site to be reopened to the usual heavy vehicle traffic.

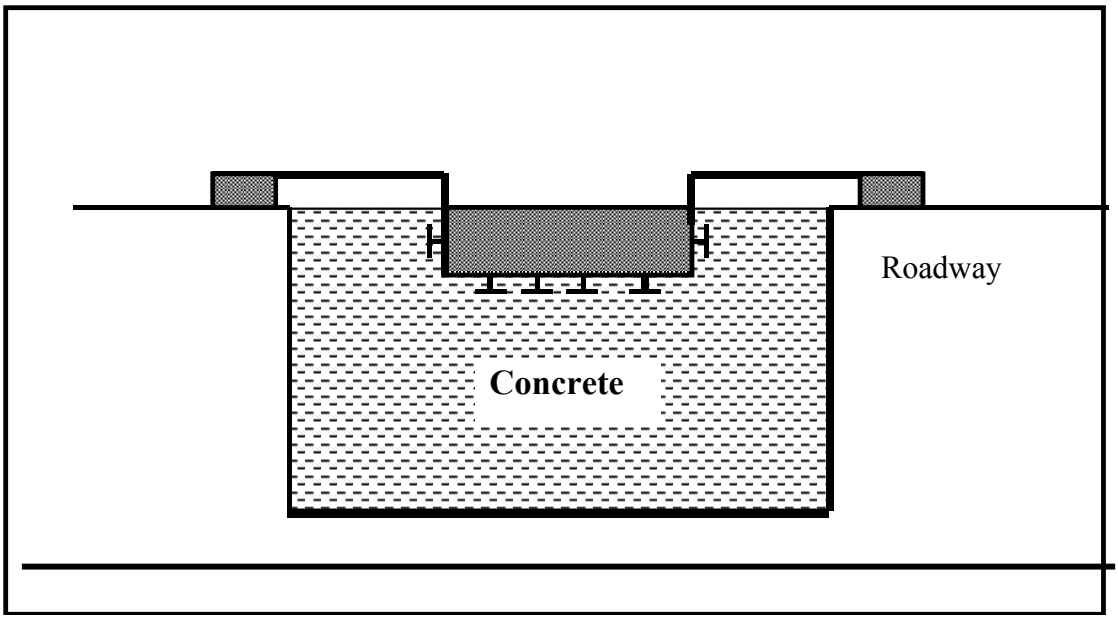

Figure 17 – Diagram of the support base for the trial slab

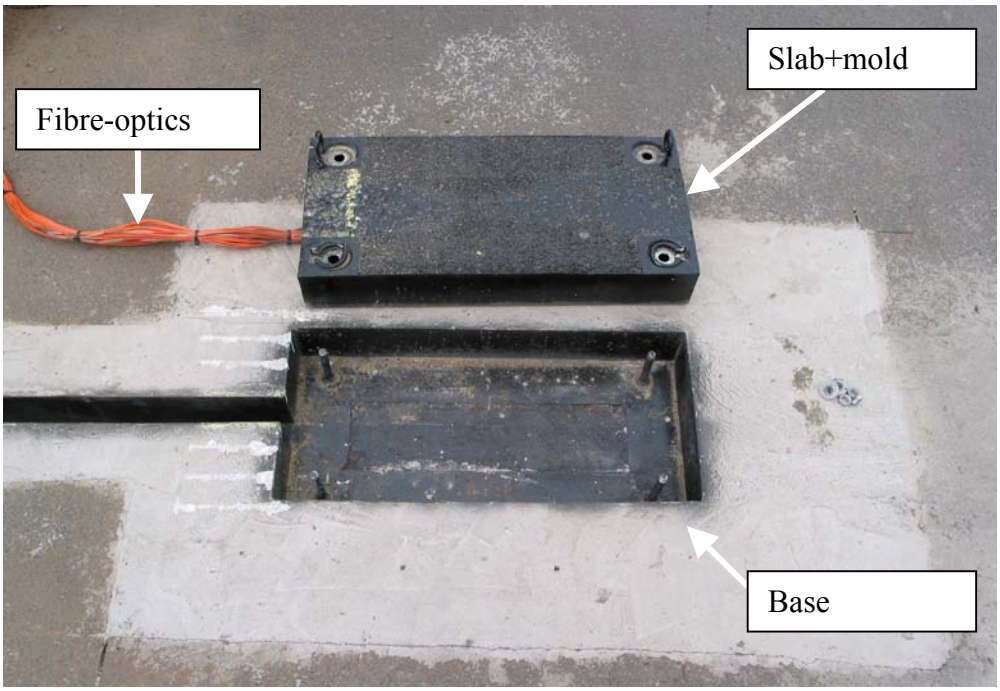

Figure 18 -- Epoxy/aggregate slab outside the support base

By placing gauges in the slab, it was possible to obtain distortion readings at 25 mm of depth and in a material whose behaviour approximated that of asphalt concrete.

4. MEASUREMENTS

4.1. Experimental protocol

The goal of this study was to measure the deflections and distortions at various levels in the roadway under various stress conditions. A roadway's stress conditions vary with the period when readings are taken, i.e. in the spring when thawing is underway or during the summer when the roadway is free of frost, and with the configurations used to conduct the trials. The configurations were obtained by varying the tire types, loads, and inflation pressures. Fifteen configurations were tested during the trials using:

- Four tire types (Figure 19) were tested: dual tires 11R22.5 (Bridgestone) and 12R22.5 (Michelin), and single tires 385/65R22.5 (Michelin wide) and 455/55R22.5 (Michelin extra-wide).
- Five loads: 3,000, 4,000, 5,000, 6,000, and 7,000 kg / half axle (two dual tires equivalent to a single tire). These loads were obtained by installing 2,200 kg concrete blocks before the trials.
- Three inflation pressures: 560, 730, and 900 kPa. These inflation pressures were chosen to cover the range of commonly used pressures.

Figure 19 - The four tire types tested (from left to right): 11R225, 12R22.5, 385/65R22.5 and 455/55R22.5

The spring and summer trials were conducted as follows for each load:

- Distortions and deflections were measured as the Benkelman vehicle passed. Temperature readings were then taken at various levels in the roadway by the thermistors (Figure 8);
- Concrete blocks were placed on the truck trailer (Figure 20) as indicated in Appendix 4;
- Tire loads were checked by placing portable scales under each tire on the trailer's two back axles (Figure 21). These readings were taken near the instrumented area to reproduce load conditions for each tire identical to those occurring as the vehicle moved over the sensors;
- A tire print was taken;
- Tire height was measured;
- Distortions and deflections were measured during two valid passes by the truck at 50 km/h. A pass was validated when the centreline of the right outside wheel on the trailer's first axle coincided with the centreline of the deflectometer, with 50 mm of offset allowed. For practical reasons during the trials, a marker was painted on the roadway to monitor the discrepancy between the outside edge of the tread and the ideal position (Figure 22). The discrepancy was estimated and noted for each valid truck pass;
- Tire pressures were reduced to 730 kPa, then to 560 kPa. The following steps (taking a tire print, measuring tire height, measuring distortions and deflections) were repeated for the two other inflation pressures.

Figure 20 – Truck used for the trials

Figure 21 – Portable scales placed under the truck's wheels to measure the load

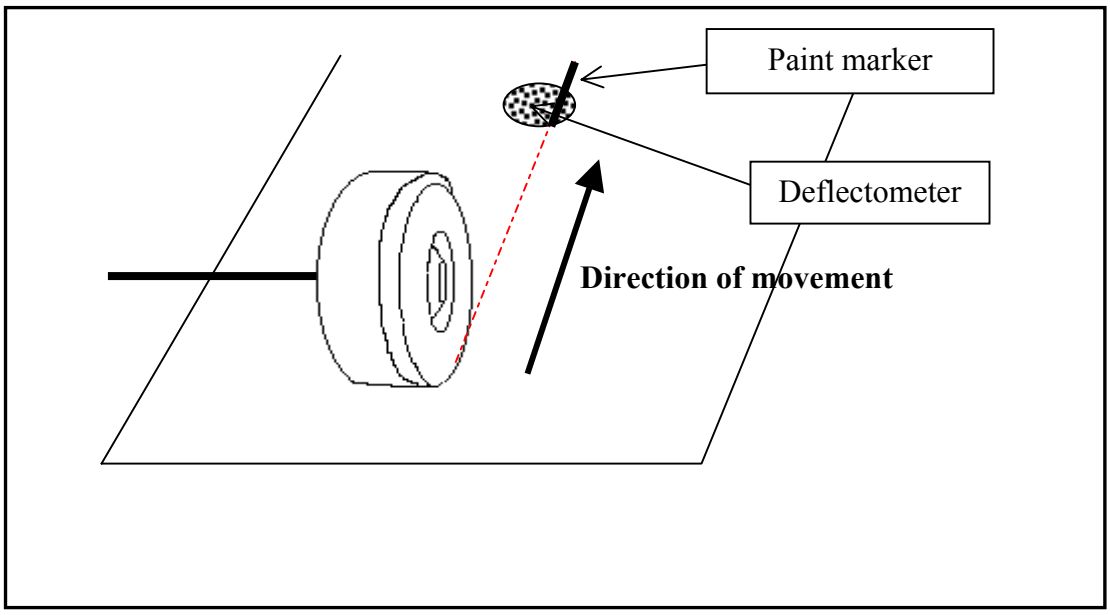

Figure 22 - Evaluating the discrepancy between the wheel's centreline and the deflectometer's centreline

The distortions and deflections caused by the Benkelman vehicle (Figure 23) were measured every sixth pass of the truck, to serve as a control. Here are the Benkelman vehicle's specifications:

- Type of axle: single with dual tires;
- Axle load: 8,165 kg;
- tire type: radials with a 203 mm tread (11R22.5)
- tire pressure: 550 kPa

Figure 23 - Benkelman vehicle

4.2. Measuring deflections and distortions in the roadway

First, the loads on the tires were checked with portable scales as each new load was placed on the truck. The readings for the spring trials are presented in Appendix 5 (tables A5.1, A5.3, A5.5, and A5.7) and those for the summer trials in Appendix 6 (tables A6.1, A6.3, A6.5, and A6.7). What emerges is that, despite the slight incline on the site (3.05 %), the load readings were close to the target values, especially for the wheel used for this study, namely the outside wheel on the first back axle (scale 1). This is why the theoretical half-axle loads (3,000, 4,000, 5,000, 6,000, and 7,000 kg / half-axle) were used in processing the findings.

The temperature readings taken during the passes by the Benkelman vehicle are presented in Appendix 7. The spring pavement temperature readings (Table A7.1) showed a temperature change over the course of a day of approximately 5ºC, except for May 8, 2002 (trials with 385/65R22.5 tires and the trial with the 7,000 kg/half-axle load on 12R22.5 tires) when a difference of 15ºC was observed between the start and end of the day. The thermistors placed at various levels in the roadway identified an area where the temperature was very close to 0ºC at 1,500 mm of depth (figures A7.1 and A7.2), probably indicating that a layer in the subgrade remained frozen during the spring. During the summer (Table A7.2), the average roadway temperature was approximately 20°C during the trial period, with minor variations in the order of 5°C. A variation of 10°C was nevertheless recorded on July 11, 2002. The temperatures over the entire roadway structure were equally constant, especially at lower depths (Figure A7.2).

Temperature should therefore have a minimal impact on the variations in readings recorded during this period.

The signals from the multilevel deflectometer movement sensors and the distortion gauges at the pavement base were transmitted over fibre-optic cables (Doré and Duplain, 2002). A specific data collection system was therefore required. This system consisted of a device for sending and receiving light signals (BUS device) and a laptop computer for recording the readings using data collection software (Figure 24). The data were collected at a frequency of 500 Hz.

Figure 24 - Distortion gauge and multilevel deflectometer data collection system

The computer recorded the deflectometer data as files containing deflection readings correlated to time. Typical signals captured by the multilevel deflectometer are presented in Figure 25. The first three peak readings correlate to the tractor's single and double axles; the next two correlate to the trailer's two back axles. Each curve reflects the readings taken by one of the four deflectometer plates.

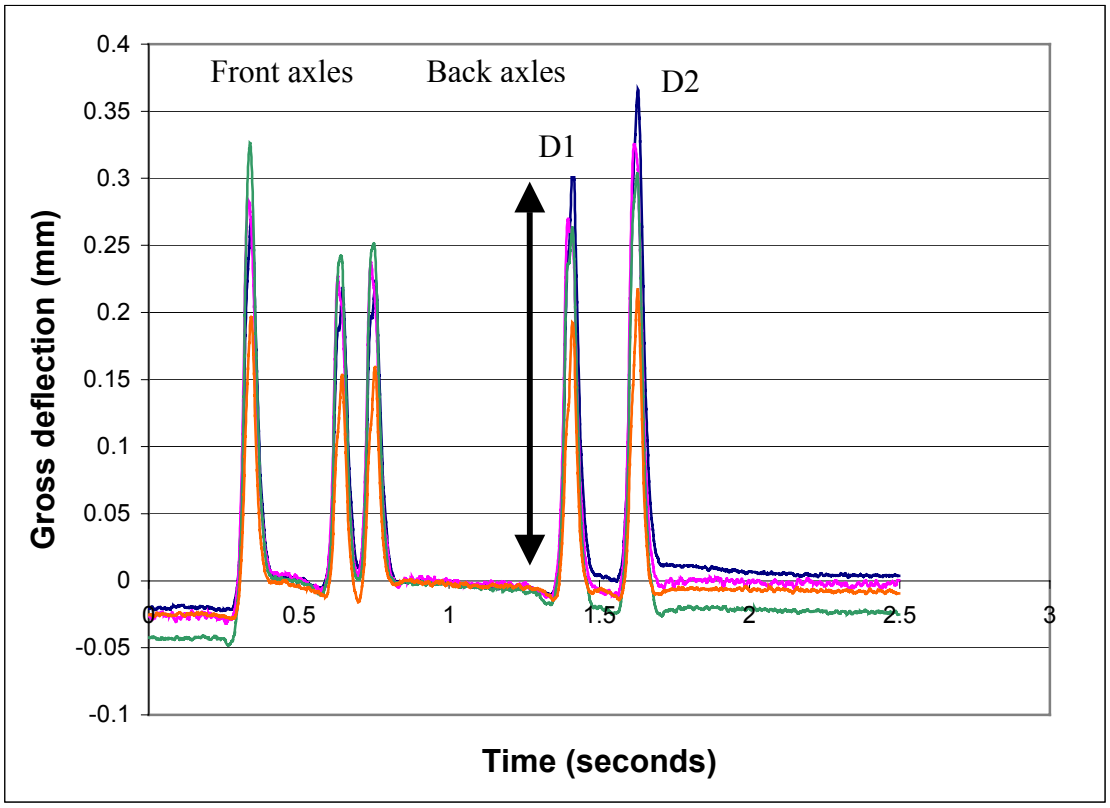

Figure 25 - Typical signal obtained from the multilevel deflectometer

The readings used in this study were taken from the first back axle on the trailer, which is why the readings were reset to zero before the fourth peak, to cancel the effects of the other axles. Based on curves of the same type as those presented in Figure 25, the maximum deflection values for each deflectometer plate (peak values D1 and D2 on Figure 25) that correlate to the passing of the truck's two back axles during the spring trials were compiled in Appendix 8, tables A8.1 to A8.4, and in tables A8.5 to A8.8 for the summer trials. All the data were checked to eliminate inconsistent values based on significant differences between peak values for two passes and on tire centre offset in relation to the centre of the multilevel deflectometer read head (tables A5.2, A5.4, A5.6, and A5. 8 for the spring trials and A6.2, A6.4, A6.6, and A6.8 for the summer trials).

The computer recorded the data from the distortion gauges at the pavement base as data files containing distortion readings correlated to time (same process as for the deflection readings). The distortions were measured in two directions, longitudinally and transversally in relation to the truck's direction of movement. According to some researchers, lateral stresses (transversal) initiate fatigue cracks and longitudinal stresses extend and open these (Owende *et al.*, 2001). The typical signal for longitudinal distortions is presented in Figure 26 and for transversal distortions in Figure 27.

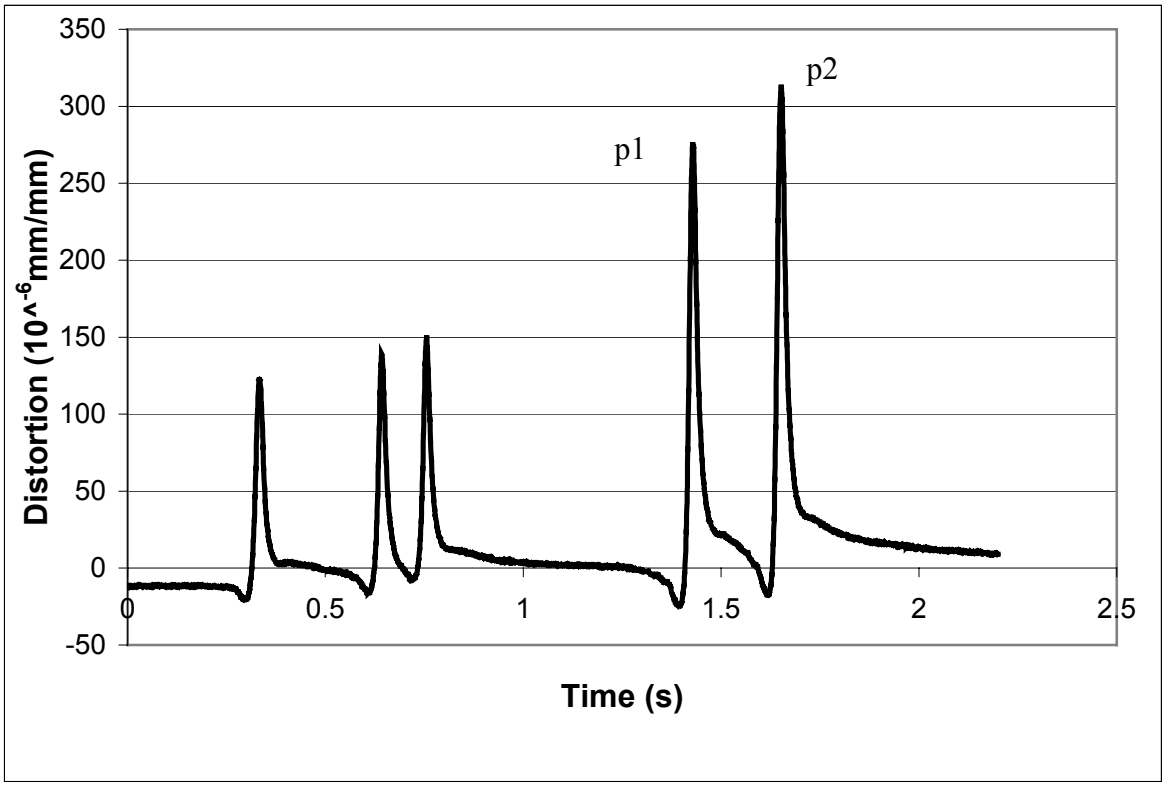

Figure 26 – The typical obtained from the longitudinal distortion gauges

The curves each show five distortion peaks that correlate to the truck's axles as they pass. Since the stresses are directly proportional to the distortions, the curve in Figure 26 shows the appearance of light compression stresses (negative values) as the wheels approach, and the

development of traction stresses (positive values) as the wheels pass by. Each pass of a wheel is considered independent because the stresses involved dissipate rapidly. On the other hand, the transversal stresses (Figure 27) dissipate slowly; this phenomenon is associated with the viscoelastic behaviour of the pavement layer (Owende *et al.*, 2001). The maximum values for longitudinal and transversal distortions (peak values p1 and p2 on figures 26 and 27) correlating to the two back axles were compiled in Appendix 9, tables A9.1 to A9.4, for the spring trials and tables A9.5 to A9.8 for the summer trials.

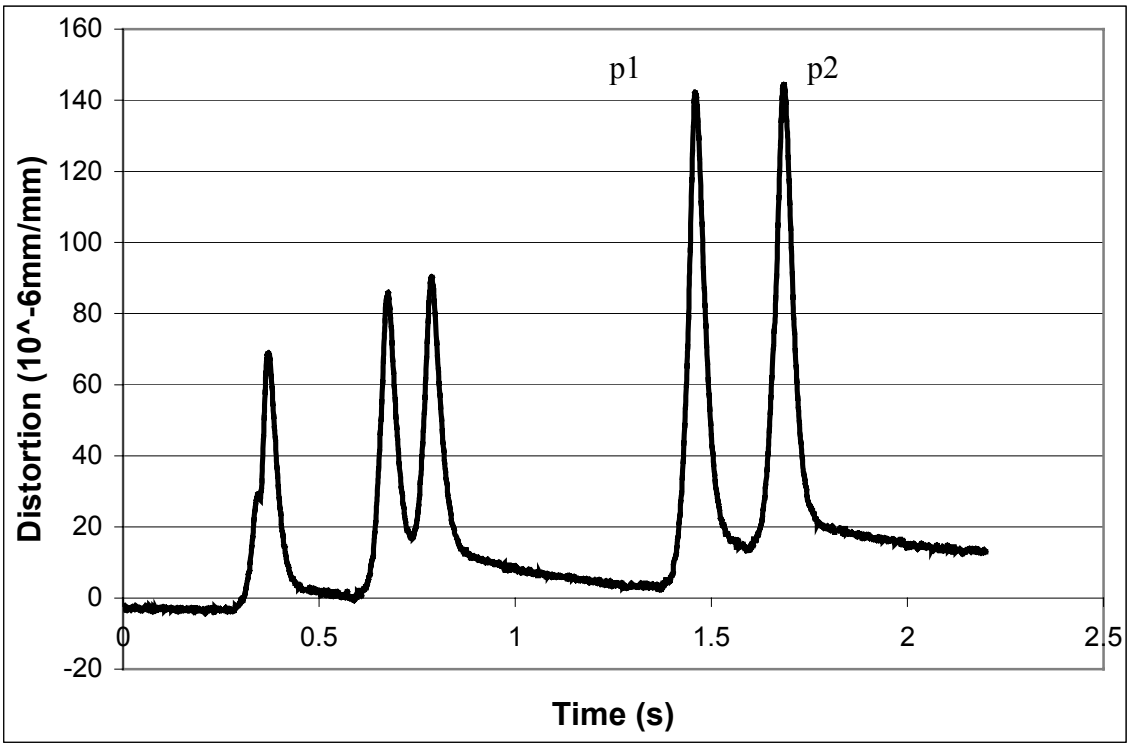

Figure 27 - Typical signals obtained from the transversal distortion gauges

4.3. Measuring distortions in the pavement

Pavement distortion readings from the instrumented slab were taken for each configuration, i.e. for the four tire types, five loads (3,000 to 7,000 kg/half-axle), and three tire pressures (560, 730, and 900 kPa). As well, the readings were also taken by having the Benkelman vehicle pass over the slab with each change of load.

Since the purpose of taking these readings was to study how asphalt pavement behaves as a wheel passes, readings were not only taken directly over the distortion gauges but also before and after, to simulate the tire's approach and departure. Therefore, for each configuration, distortion was monitored with the tire at eight different positions on the slab—with the midpoint of the tire at the edge of the slab and then at 5 cm intervals. To take the readings in a consistent fashion, lines 5 cm apart were drawn on the slab and on the outside wall of the tire. It was then necessary to match up the two series of lines as the wheel passed (Figure 28). The tire's lateral position on the slab was monitored by aligning the edge of the tread with another marker 75 mm from the edge of the slab. Thus, distortions were measured even outside the area of tire/slab contact, which

facilitated studying roadway behaviour at the edges of tire. As well, apart from readings taken with tires on the slab, distortion gauge readings were taken with no truck, i.e. with no load stress on the slab. These readings constitued the control trials.

The slab readings were obtained under quasi-static condition. The data collection system needed a delay of a few minutes to read each channel several times (five on average). The readings were recorded using two devices sending and receiving light signals over fibre-optic cables. These devices (32-channel DMI and 4-channel UMI) were directly linked to laptop computers for data capture (Figure 29). The data were compiled in the form of nine files (a "zero" file and eight files containing readings) for each monitoring device and each configuration. As well, there was a one-minute delay before recording data for each tire position to allow the distortion gauges to stabilize after being disturbed by advancing the vehicle and, in particular, braking to position it over the slab.

Figure 28 – Tire advancement control procedure

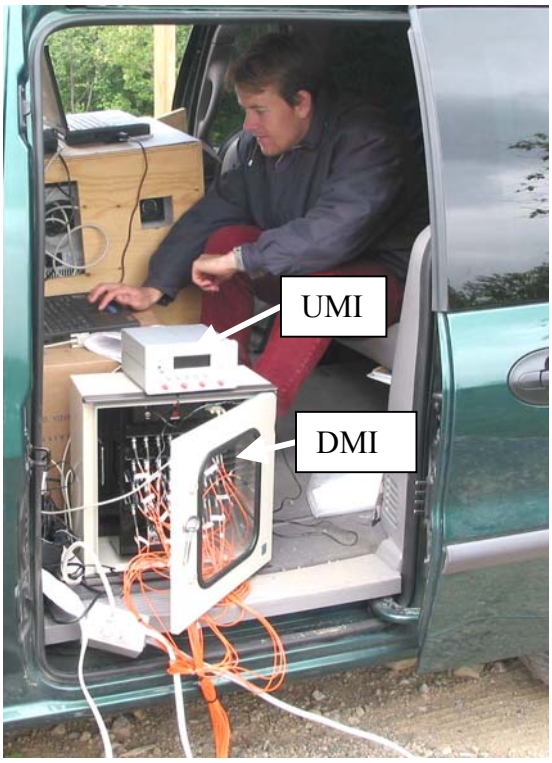

Figure 29 – Fibre-optic slab gauge data collection system

To provide an example, the slab distortion values for the 11R22.5 tire are compiled in Appendix 10. The values in these tables represent the average of the three highest values obtained for each tire position on the slab for each configuration.

Concurrent to these distortion readings, slab temperature readings were taken by four thermistors. These values are presented in Appendix 11, Table A11.1, and they represent the average of the four readings obtained. The purpose of these readings was to determine how heat changed the behaviour of the epoxy/aggregate mix under real-life conditions, and to make corrections if necessary.

4.4. Other measurements

Tire height was determined using a digital vernier. These measurements were taken with the tire on the roadway flattened under the weight of a load, and with the tire on a free wheel (Figure 30). The tire height values are provided in Appendix 12.

The free wheel measurements did not reveal a clear trend in tire behaviour. This was due to the fact that it was difficult to have the tire touch the ground, using the roadway as a control surface, without the tire flattening. However, it was determined that a tire's height is greater on a free wheel than when it is flattened under the weight of a load. In addition, the flattened tire data revealed the two following points: tire height decreases as the load increases, and, under equivalent loads, tire height decreases as the inflation pressure decreases.

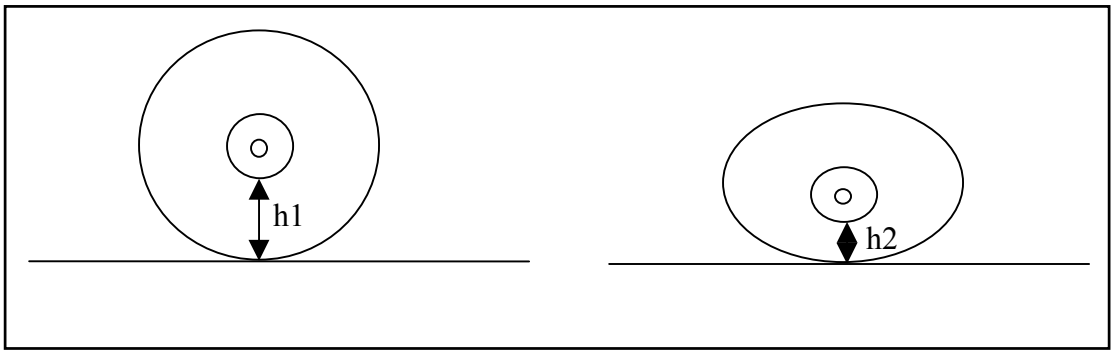

Figure 30 – Measuring tire height *h*: on a free wheel (h1) and flattened on the roadway (h2)

To obtain prints, tires were covered with paint and then pressed onto a piece of paper (Figure 31). Tire prints were taken for each configuration during the spring trials but only once per tire (at 1,500 kg/tire and 900 kPa) during the summer trials for control purposes. The tire contact area on the roadway was measured using the tire prints. Samples of each tire type are shown in Appendix 13. The surface areas of the tire prints are given in Appendix 13. The gross area correlates to the tire print on the roadway, including the spaces between the ribs, while the net area may be associated with that of a smooth tire, without treads. Is is clear that greater loads increase the tire-pavement contact area. This observation applies irrespective of inflation pressure.

Figure 31 - Taking a tire print

5. PRESENTING AND ANALYSING THE FINDINGS

5.1. Roadway behaviour

Roadway response parameters may be defined to assist in evaluating the effects that tires have on roadway behaviour. A flexible roadway, like the one at the SERUL site, undergoes two types of degradation: fatigue cracks and rutting (Sebaaly, 1992). Maximum stresses on the pavement base cause fatigue cracks, and accumulated vertical stresses at the topgrade cause rutting (Figure 32). Most studies on this subject (Owende *et al.*, 2001) define roadway damage in terms of fatigue cracks and rutting.

This is why this study first evaluated these parameters by measuring distortions at the pavement base and at the topgrade to compare the distortion effects for each tire type. The study then looked at the pavement distortions responsible for creep rutting.

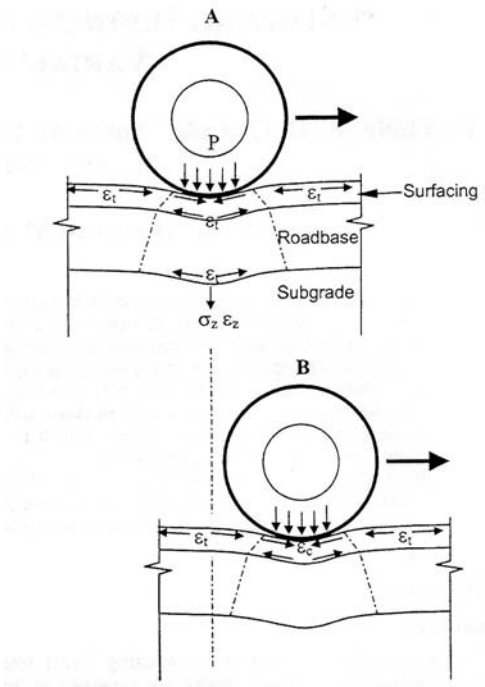

Figure 32 - Roadway response as a wheel reaches two successive positions (Owende *et al.*, 2001)

5.2. Distortions at the topgrade

The purpose of this part of the study was to evaluate the impact that various tires have in terms of topgrade distortions. The readings taken by the multilevel deflectometers provided this information. The multilevel deflectometers consisted of four plates situated at various depths in the roadway. Plates 2 and 3 were located at depths of 1,100 and 800 mm, respectively. The layer between these two plates was the top 300 mm of the subgrade. Deflections in this layer were captured by subtracting the values registered by the lead at the top of this layer from the values registered by the lead at the bottom, i.e. "deflectometer 2 -- deflectometer 3." The distortion value

was then obtained by dividing the deflection in this layer by the layer's thickness, namely 300 mm. The following equation was applied to obtain distortions at the topgrade:

$$distortion = \frac{peak\ values\ deflectometer\ 2 - peak\ values\ deflectometer\ 3}{300\ mm}$$

It should be noted that before the deflections were transformed into distortions, they were standardized in relation to the Benkelman vehicle. First, the gross deflection peak values that occurred in the roadway as the Benkelman vehicle passed were correlated in graphic format to the temperatures readings. The trend curve equation identified the theoretical deflection values caused by the Benkelman vehicle using the temperature reading taken with each load (Table 2). The gross deflections for the various tires were then divided by the theoretical values for the Benkelman vehicle at the same temperature, namely the temperature at which the trial was conducted. Through this calculation, the deflection values were adjusted to reflect factors external to roadway behaviour itself, such as temperature. These theoretical deflection values for the Benkelman vehicle were also used to integrate the variations in readings caused mainly by offset of the wheel on the multilevel deflectometer read head.

Table 2 – Deflection trend line equations related to temperature

	Trend curve equation
Deflectometer 1	$D = 0.2857\ e^{0.0075T°}$
Deflectometer 2	$D = 0.2654\ e^{0.002T°}$
Deflectometer 3	$D = 0.2625\ e^{0.0065T°}$
Deflectometer 4	$D = 0.1792\ e^{0.0006T°}$

In the spring, the deflection values registered by deflectometer 2 were higher than those registered by deflectometer 3, except for a few series of readings. Standardized distortions at the topgrade were nevertheless calculated and are presented in tables A14.1 to A14.4 in Appendix 14. The wide variation in distortion values, probably due to the fact that a layer of the subgrade remained frozen during the spring, made it difficult to compare how the various tire types affect topgrade distortions. In the summer, a majority of deflectometer 3 values were higher than the deflectometer 2 values. The wide variation in standardized distortion values obtained during the summer trials (tables A14.5 to A14.8 in Appendix 14) also hindered drawing conclusions on what occurs at the topgrade, even if the topgrade distortions appear to increase slightly as loads increase. However, in both the spring and summer, the order of magnitude of the findings as whole presented in tables 14.9 to 14.16 indicates that the distortions affecting lower levels of the roadway are very weak, almost nil. Furthermore, these topgrade distortions do not appear related to tire type, inflation pressure, or even load.

5.3. Distortions at the pavement base

Distortions at the pavement base as well as the calculations performed on these readings for the spring and summer trials are presented in Appendix 15. For both these trial periods, only the higher of the two distortion values at the pavement base, i.e. longitudinal or transversal, was used in analysing the most critical distortion in terms of fatigue cracks. Similarly, the higher distortion values at the pavement base, i.e. longitudinal or transversal, recorded during a pass by the Benkelman vehicle was used. The trend curve equations that generated theoretical distortion values for the Benkelman vehicle at the same temperature at which the trial was conducted with the various tire types are presented in table 3.

Table 3 – Distortion trend curve equations related to temperature

	Trend curve equation
Longitudinal distortions	$D = 109.83\ e^{0.0266T°}$
Transversal distortions	$D = 39.895\ e^{0.0489T°}$

The maximum distortion values at the pavement base are contained in Appendix 15 (tables A15.1, A15.4, A15.7, and A15.10 for the spring trials and A15.13, A15.16, A15.19, and A15.22 for the summer trials). These distortions were then transformed into a number of load applications (N) using the Asphalt Institute fatigue model:

The N values calculated with this model are presented in tables A15.2, A15.5, A15.8, and A15.11

$$\varepsilon_R = K\left(\frac{N}{10^6}\right)^{\left(\frac{-1}{a}\right)} \quad with\ K = 240\ and\ a = 3.29$$

for the spring trials and tables A15.14, A15.17, A15.20, and A15.23 for the summer trials. The $N_{Benkelman}/N_{trial}$ ratio was then calculated for the various tire types and loads. The values calculated are presented in tables A15.3, A15.6, A15.9, and A15.12 for the spring trials and A15.15, A15.17, A15.21, and A15.24 for the summer trials.

To analyse the findings more easily, the values for pavement base distortions, various tire types, and various loads were only presented graphically (figures 33 and 34) for the 730 kPa inflation pressure, the one most commonly used by carriers. Furthermore, the linear trend curves were drawn and the distortion values calculated (tables 4 and 5), based on the equations found, for the allowable loads, i.e. 15,500 kg or 3,875 kg/half-axle in the spring and 18,000 kg or 4,500 kg/half-axle in the summer.

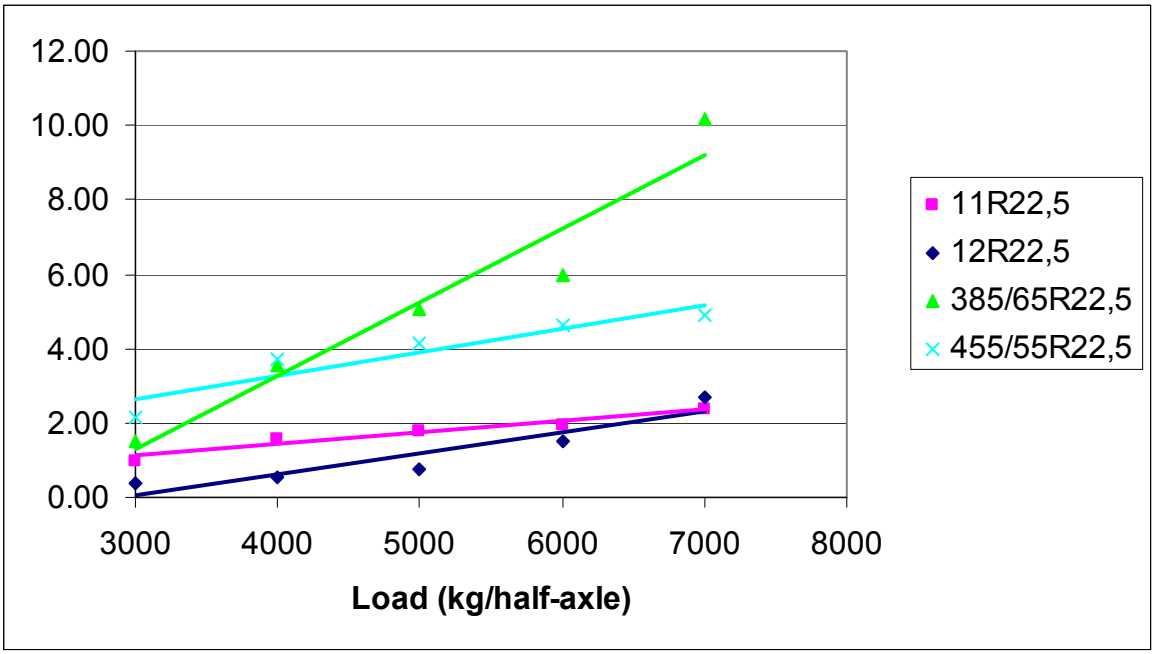

Figure 33 - $N_{Benkelman}/N_{trial}$ ratio corresponding to the distortions at the pavement base in relation to load per half-axle at a pressure of 730 kPa (spring trials)

Table 4 - $N_{Benkelman}/N_{trial}$ ratio corresponding to distortions at the pavement base at a pressure of 730 kPa (spring trials)

		Load (kg/half-axle)		
		2,875	3,875	4,875
tire type	trend curve	$N_{Benkelman}/N_{trial}$		
11R22.5	$y = 0.0003\ x + 0,1859$	1.05	1.35	1.65
12R22.5	$y = 0.0006\ x - 1,6314$	0.09	0.69	1.29
385/65R22.5	$y = 0.002\ x -- 4,6566$	1.09	3.09	5.09
455/55R22.5	$y = 0.0006\ x + 0,6972$	2.42	3.02	3.62

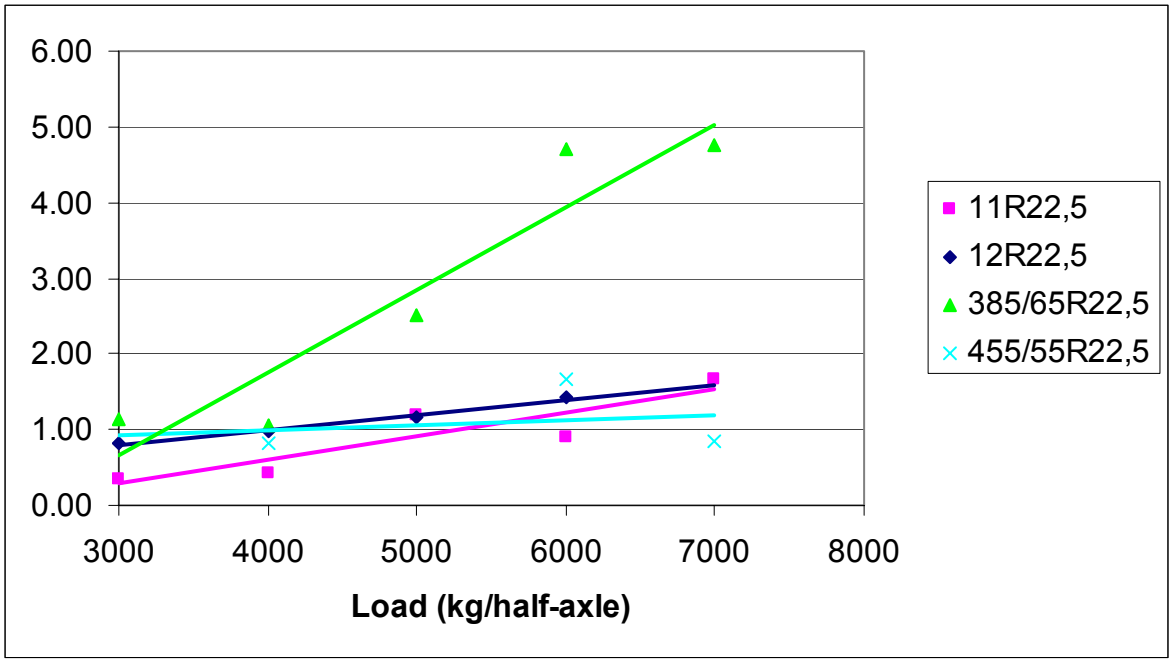

Figure 34 - $N_{Benkelman}/N_{trial}$ ratio corresponding to the distortions at the pavement base in relation to load per half-axle at a pressure of 730 kPa (summer trials)

Table 5 - $N_{Benkelman}/N_{trial}$ ratio corresponding to the distortions at the pavement base at a pressure of 730 kPa (summer trials)

		Load (kg/half-axle)		
		3500	4500	5500
tire type	trend curve	$N_{Benkelman}/N_{trial}$		
11R22.5	$y = 0.0003\,x - 0.6518$	0.40	0.70	1.00
12R22.5	$y = 0.0002\,x + 0.2084$	0.91	1.11	1.31
385/65R22.5	$y = 0.0011\,x - 2.6179$	1.23	2.33	3.43
455/55R22.5	$y = 0.00007\,x + 0.7306$	0.98	1.05	1.12

In the spring, both types of dual tires 11R22.5 and 12R22.5 create less distortions at the pavement base than the two types of wide tires. Nevertheless, the 455/55R22.5 extra-wide tire creates less distortions at the pavement base than the 385/65R22.5 wide tire. The slope of the curves tends to be positive, i.e. in general, the distortions grow with the loads the tires carry. As well, both types of dual tires and the extra-wide tire create distortions at the pavement base of the same order of magnitude in the summer.

Comparing spring and summer distortion gauge data, i.e. figures 33 and 34, yields road-friendliness observations with respect to fatigue cracks and different tire types in relation to load.

In the spring and summer, dual tires are always more road-friendly than the 385/65R22.5 wide tire, which is always the least road-friendly. This wide tire shows very little road-friendliness in the spring and slightly more in the summer. However, it is much less road-friendly, in terms of distortions at the pavement base, than the 455/55R22.5 extra-wide tire. Indeed, it is important to note that in the spring, the extra-wide tire is much more road-friendly than the ordinary wide tire, even if it is less road-friendly than both types of dual tires, but that in the summer, Figure 34 clearly shows that the extra-wide tire is comparable in terms of road-friendliness to the dual tires. It is unlikely that this finding stems from measurement errors because the $N_{Benkelman}/N_{trials}$ ratios are close to 1 for the dual tires.

From the point of view of fatigue cracks, the dual tires are less damaging to the roadway than the wide tires in the spring, although the 455/55R22.5 extra-wide tire is less damaging than the 385/65R22.5 wide tires. However, in the summer, the dual tires and the extra-wide tire are equally road-friendly and the wide tire remains very damaging to the roadway.

5.4. Vertical distortions in the pavement

Data processing began by creating tables containing the average readings for each vertical gauge and for each trial, i.e. for the eight tire positions and for the control trial. The values obtained for the control trial were subtacted from the average distortion values for each gauge recording tire stress.

The graphs resulting from these tables show the distortions in relation to distance, with each curve corresponding to a tire position. Representative graphs are presented in Appendix 16. The first one, Figure A16.1, reflects readings for the 12R22.5 tires with a load of 3,000 kg/half-axle and for an inflation pressure of 560 kPa. The curves show that as the tire advances, the compression distortions (negative values) increase. It should be noted that as a tire nears a gauge, positive values appear, signifying that traction stresses are being created. The tire's position on the slab is clearly visible through the shape of the curves. Indeed, it can be seen that at approximately 70 mm from the edge of the slab, the distortions increase rapidly, then decrease toward the centre of the tire, and finally increase again at the other edge of the tire. This characteristic appearance is due to the fact that with a low pressure, even a light load, the stresses tend to distort a tire's shape and to be distributed on its sides (Yap,1989). The "M" shape at the centre of the tire reflects the different stresses applied to the ribs of the tire. Indeed, it has been shown (Douglas *et al.*, 2000) that with a light load and at a low pressure, the stresses are greater under a tire's outside ribs and much weaker under the central rib, although the compression stresses are slightly higher under the central rib.

With high inflation pressures (900 kPa in our case), stresses are distributed differently, as shown in Figure A16.2. This graph shows the distortions created by a 385/65R22.5 tire loaded with 3,000 kg/half-axle and inflated to a pressure of 900 kPa as it passes over the slab. The curves in this case look quite different. The tire print is wider due to the tire's size and the maximum distortions are not at the edge of tire, as was seen previously, but at its centre. The study by Douglas *et al.* (2000) also showed that, at high inflation pressures, compression stresses are at their maximum level under the tire's central rib, which confirms the readings obtained from the slab. It therefore appears that, given the shape of the curves, the observations from the study by Douglas *et al.*(2000) with respect to contact pressures between tire and roadway are applicable to the stresses that develop 2.5 cm into the pavement. In Figure A26.2, for the wide tire, much weaker distortions can be observed on each side of the tire and outside the tire/slab contact area;

this phenomenon reflects the upward movement of pavement material on both sides of the tire in response to pavement compression under the tire.

Based on the readings obtained from the distortion gauges, the average of the three maximum vertical distortion values was compiled for each configuration (Appendix 17), which made it possible to draw other graphs comparing the slab's response to the stress exerted by the various tires tested. Figures 35 to 37 present the maximum distortions detected in the slab for the different tire types in relation to load and the three inflation pressures. The figures show that distortions increase as loads increase, irrespective of the inflation pressure in question. As well, for both the lower pressures (560 and 730 kPa), the trend curves for the various tire types are fairly similar and all maximum distortion values are under 200 x 10^{-6} mm/mm. For the highest pressure, i.e. 900 kPa, both the 385 and 455 wide tires have the lowest distortion values and the 11R22.5 dual tire imposes the highest distortion values.

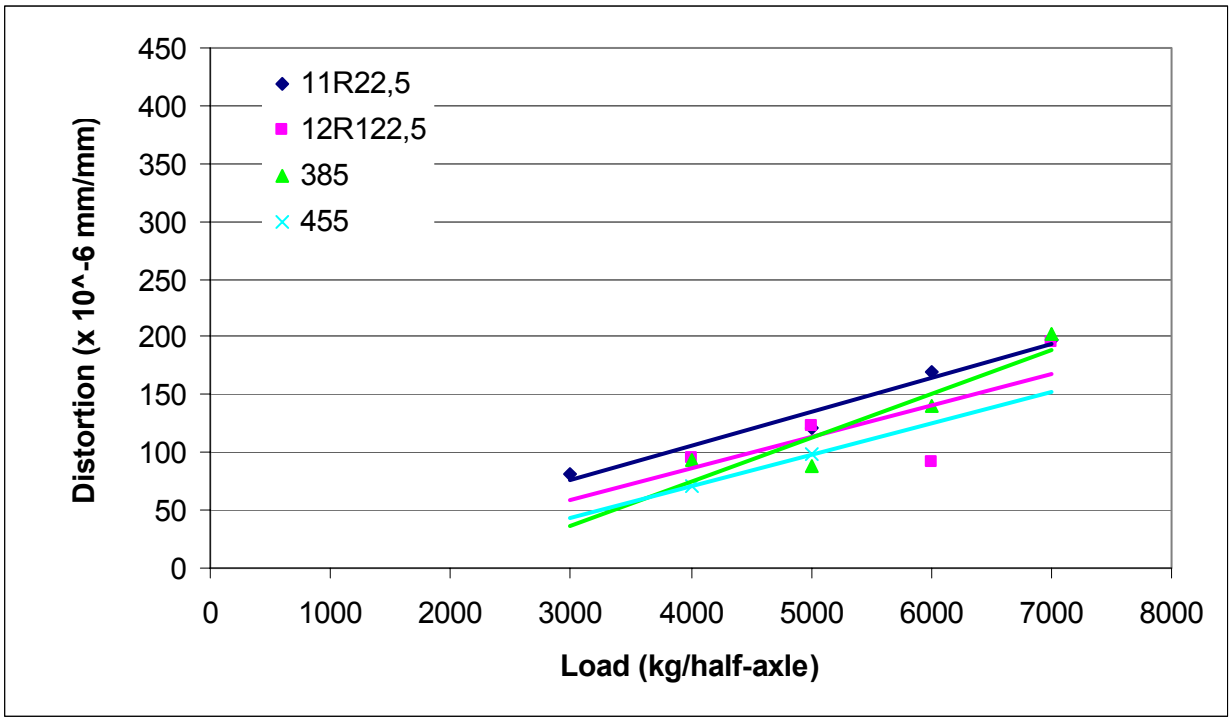

Figure 35 – Maximum distortions in relation to load at 560 kPa pressure

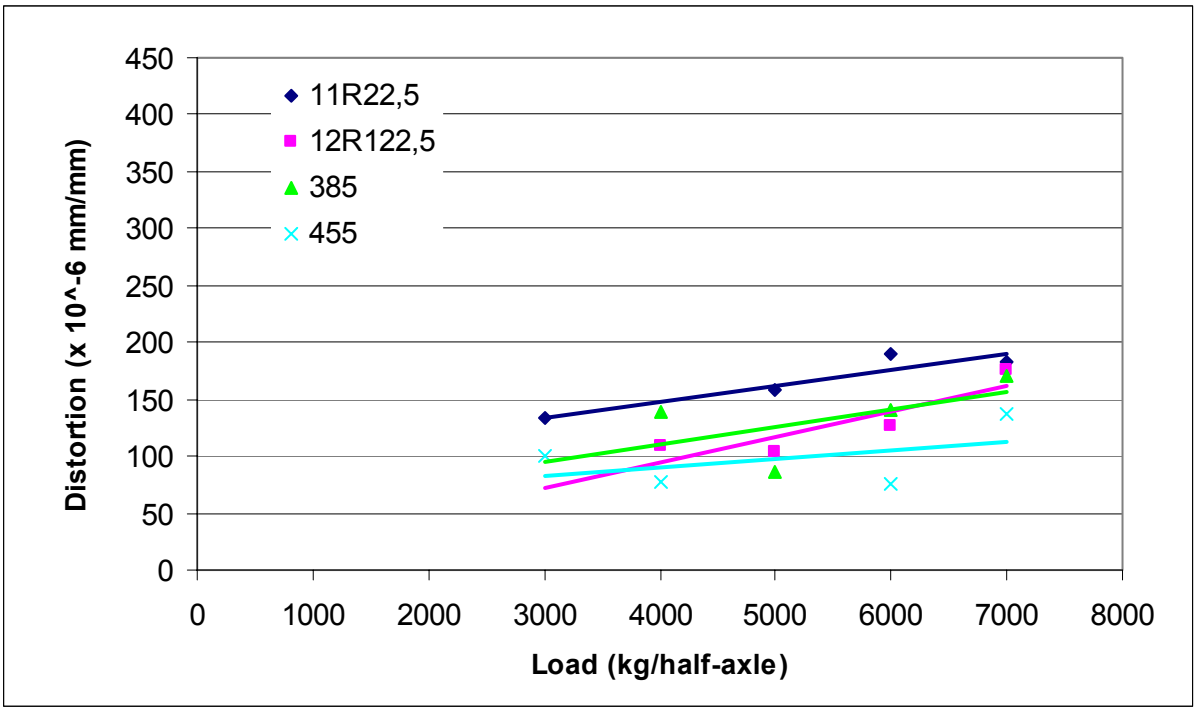

Figure 36 – Maximum distortions in relation to load at 730 kPa pressure

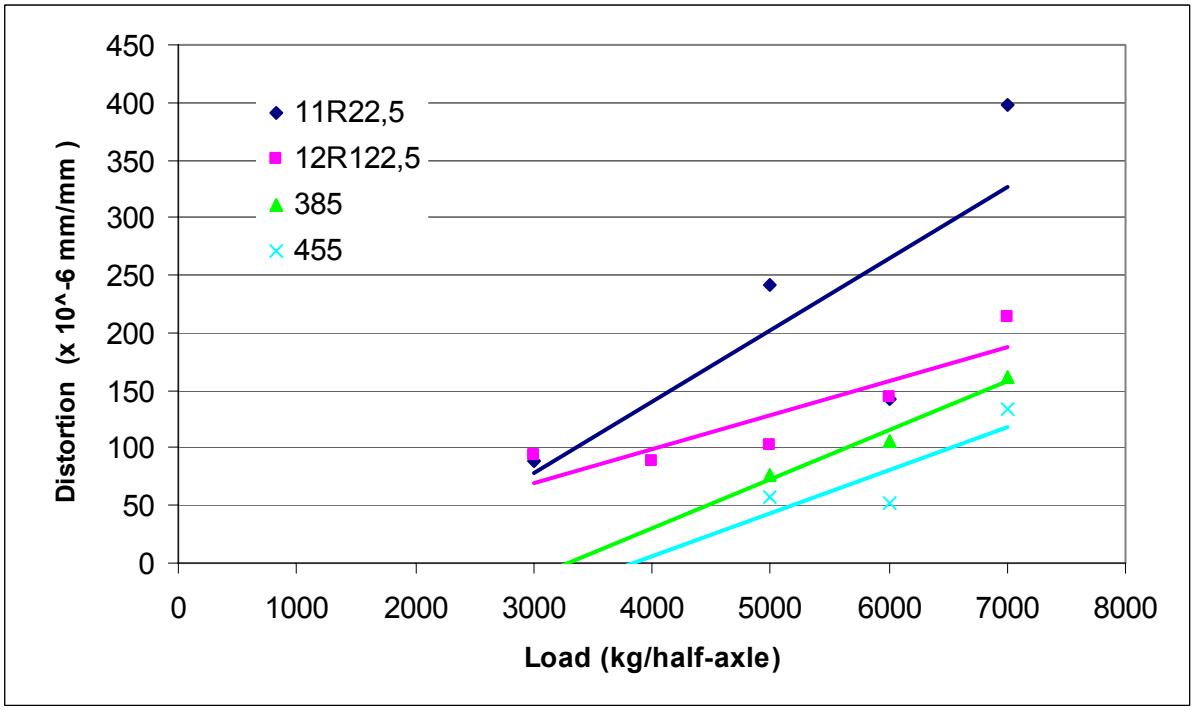

Figure 37 – Maximum distortions in relation to load at 900 kPa pressure

Furthermore, based on figures 35 to 37, the linear trend curves equations were used to calculate the maximum distortion values for the allowable load in the summer, i.e. 18,000 kg or 4,500 kg/half-axle. Based on the following equation (AASHTO 2002):

with temperature (T) and set number of load applications (N), permanent distortion is directly

$$\log\left(\frac{\varepsilon_p}{\varepsilon_r}\right) = -3.74938 + 0.4262\ \log(N) + 2.02755\log(T)$$

related to the reversible distortion recorded. Table 6 gives tire distortion ratios with the 11R22.5 dual tire taken as a reference. These figures may be analysed in terms of permanent distortions causing creep rutting.

Table 6 – Distortion ratio ($\varepsilon_{trial}/\varepsilon_{11R22.5}$) for a load of 4,500 kg/half-axle

	Pressure		
	560 kPa	730 kPa	900 kPa
11R22.5	1	1	1
12R22.5	0.83	0.68	0.67
385/65R22.5	0.78	0.76	0.30
455/55R22.5	0.70	0.60	0.15

The values calculated for an allowable load of 18,000 kg decrease as inflation pressures increase for all tires. Both dual tires caused the greatest pavement distortions. Both wide tires and especially the 455/55R22.5 extra-wide tire caused very weak pavement distortions.

Processing the vertical distortion data revealed that high inflation pressures (900 kPa) appear to be more damaging from the point of view of vertical distortions at a pavement depth of 25 mm because the highest distortion values were measured at this inflation pressure. The 560 and 730 kPa pressures appear to produce the smallest distortions. Comparing all the graphs indicates that the 455/55R22.5 extra-wide tire causes the least pavement distortion, especially at high inflation pressures, followed by the 385/65R22.5 wide tire and the 12R22.5 dual tires, which both cause similiar distortions at the 560 and 730 kPa inflation pressures. With respect to the 11R22.5 dual tires, they appear to be the most damaging to the pavement in many configurations.

6. CONCLUSION

The goal of this research project was to obtain data related to vehicle movement over a roadway, for several configurations and at various levels in the roadway. The innovative data obtained from an instrumented slab provided roadway behaviour information that was more complete in comparison to the readings taken at the pavement base and topgrade.

The various configurations used in the trials demonstrated, first of all, the effect that tire loads have on roadway behaviour. Increasing the load results in a systematic increase in deflections at various levels in the roadway, but also in distortions at the pavement base and in the pavement itself. Tire pressure was the second parameter studied during the trials. The data related to roadway deflections and to distortions at the pavement base showed that inflation pressure has no significant effect on these readings. Pavement distortions appear to increase with tire inflation pressure.

The last parameter considered during the trials was tire type. The differences in the roadway behaviour caused by dual tires (12R22.5 and 11R22.5) and wide tires (385/65R22.5 and 455/55R22.5) are especially marked. With respect to total roadway deflection, the dual tires are less damaging to the roadway than wide tires. Concerning distortions at the pavement base, in the spring, the dual tires are more road-friendly than wide tires, and the extra-wide tire is less damaging that the ordinary wide tire. The readings taken during the summer indicated that the 455/55R22.5 extra-wide tire and the dual tires are equally road-friendly with respect to fatigue cracks and distortions at the pavement base, while the 385/65R22.5 wide tire continues to show very low road-friendliness in this respect. The readings obtained with the instrumented slab indicated that the 385/65R22.5 and 455/55R22.5 wide tires cause less vertical distortions at a pavement depth of 25 than the dual tires.

In conclusion, this study examined pavement distortions in greater detail. It also showed that each factor or stress level associated with the various forms of roadway damage must be weighted (Figure 38). In other words:

- Vertical distortion at a pavement depth of 25 mm affects pavement creep rutting;
- Distortion at the pavement base affects roadway fatigue cracking;
- Vertical distortion at the top grade affects structural rutting of the roadway.

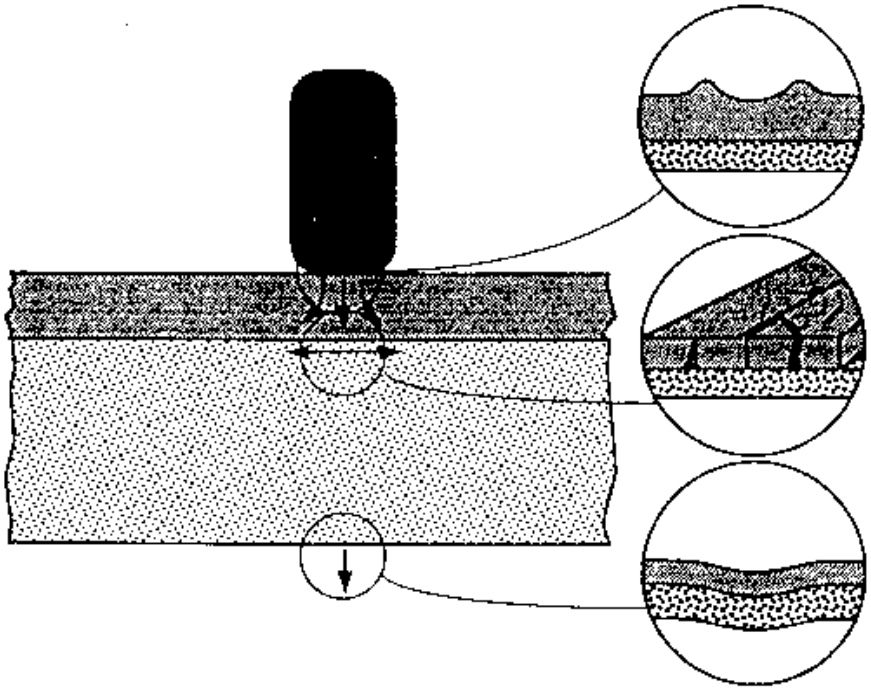

Figure 38 – Critical stress levels and associated damage

This weighting should make it possible to circumscribe dual tire and wide tire use such that roadway damage is truly minimal at all stress levels.

7. REFERENCES

PROPHÈTE, F. *Effet des largeurs de pneus*, étude 255(31)99. Service des chaussées, Secteur expertises en chaussées, Ministère des transports du Québec, 1999, 59 p.

SEBAALY, P.E. *Pavement Damage as Related to Tires Pressure, Axle Loads and Configurations*. Vehicle, Tire, Pavement Interface, ASTM STP 1164, J.J. Henry and J.C. Wambold, Eds., American Society for Testing and Materials, Philadelphia, 1992, pp. 69-96.

FINN, F. *et al. Development of Pavement Structural Subsystems.* National Cooperative Highway Research Program, Report No. 291, Transportation Research Board, Washington, 1986.

CHRISTISON, J.T. *Pavement Response to Tire Inflation Pressure.* Canadian Strategic Highway Research Program (C-SHRP), Alberta Research Council, Project No. 1260, 1990, 15 p.

OWENDE, P.M.O., HARTMAN, A.M., WARD, S.M., GILCHRIST, M.D., and O'MAHONY, M.J. *Minimizing Distress on Flexible Pavements Using Variable Tire Pressure*. Journal of Transportation Engineering, 2001, pp. 254-262.

LIPPMANN, S.A. *Effects of tire structure and operating conditions on the distribution of stress between the tread and the road.* The tire pavement interface, ASTM STP 929, edited by M.G. Pottinger and T.J. Yager, American Society for Testing and Materials, Philadelphia, 1985, pp. 91-109.

MARSHEK, K.M., CHEN, H.H., CONNELL, R.B., and HUDSON, R.W. *Experimental determination of pressure distribution of truck tire-pavement contact.* Transportation Research Record 1070, Transportation Research Board, National Research Council, Washington, 1986, pp. 9-14.

SIEGFRIED. *The study of contact characteristics between tyre and roadway*. D Phil. thesis, Department of Civil Engineering, School of the Built Environment, University of Ulster at Jordanstown, Northern Ireland. 1998.

TIELKING, J.T., and ROBERTS, F.L. *Tire contact pressure and its effect on pavement strain*. ASCE Journal of Transportation Engineering, 113(1), 1987, pp. 56-71.

DE BEER, M., FISHER, C., and JOOSTE, F.J. *Determination of pneumatic tire/pavement interface contact stresses under moving loads with some effects on pavements with thin asphalt surfacing layers.* Proceedings of the 8th International Conference on Asphalt Pavements, International Society for Asphalt Pavements, Seattle, 1997, pp. 179-227.

DOUGLAS, R.A., WOODWARD, W.D.H., AND WOODSIDE, A.R. *Road contact stresses and forces under tires with low inflation pressure.* Canadian Journal of Civil Engineering, 27, 2000, pp. 1248-1258.

DE BEER, M. *Measurement of tyre/pavement interface stresses under moving wheel loads.* Heavy Vehicle Systems, Special Issue, Vol. 3, Nos. 1-4, 1996, pp. 97-115.

KRARUP, J. *Measured and Calculated Pavement Reponse in the Danish Road Testing Machine.* Danish Road Institute, Road Directorate, Denmark Ministry of Transport, Note 236, 1992, 25 p.

HOWELL, W.E., PEREZ, S.E., and VOLGER, W. A. *The Pavement Interface*. Aircraft Tire Footprint Forces, edited by M.G. Pottinger and T.J. Yager, 1986, pp. 111-112.

TIELKING, J.T., and ABRAHAM, M.A. *Measurement of Truck Tire Footprint Pressures.* Transportation Research Record 1435, Transportation Research Board, pp. 92-99.

DORÉ, G, DUPLAIN, G. *Monitoring Pavement Response during Spring Thaw Using Fiber-Optic Sensors.* Proceedings of the 6th international conference on the bearing capacity of roads and airfields, edited by A.G. Correia and F.E.F. Branco, Lisbon, Portugal, 2002, pp.15-24.